理學博士學位論文

Mis18α에 의한 동원체 크로마틴과 CENP-A 조절에 관한 연구

Regulation of Centromeric Chromatin and CENP-A Loading by Mis18α

2012年 8月

서울大學校 大學院

生命科學部

金 益 秀

Regulation of Centromeric Chromatin and CENP-A Loading by Mis18α

by

Ik Soo Kim

Advisor

Associate Professor Sung Hee Baek, Ph.D.

A Thesis for the Degree of Doctor of Philosophy

August, 2012

School of Biological Sciences

Seoul National University

ABSTRACT

Mis18α is a component of Mis18 complex which is regulating chromosome segregation. Mis18 complex has been shown to localize to centromere from late mitosis to early G1 phase and mediates centromeric localization of a histone variant called CENP-A without physical interaction between them. Although this 'licensing' or 'priming' function of Mis18α is crucial for maintenance of centromere during cell division, underlying mechanisms are largely unknown. In this study, I investigated the physiological role of Mis18α in developmental stages using *Mis18α*-deficient mouse and the mechanisms of Mis18α regulating CENP-A deposition in centromere.

Mis18α-deficient mouse is lethal at early embryonic stages due to apoptotic cell death. *Mis18α*-deficient embryos at E3.5 showed severe defects of chromosome segregation and loss of CENP-A in centromere. *In vitro* culture study revealed the growth retardation in the inner cell mass of *Mis18α*-deficient embryo and subsequent cell death. The accumulation of missegregated chromosomes by loss of CENP-A in *Mis18α*-deficient embryo was the cause of apoptotic cell death during embryonic development. In addition, $Mis18\alpha^{\Delta/\Delta}$ MEFs was generated by Cre introduction and CENP-A loading and chromosome segregation were examined. Similar to the defects in *Mis18α*-deficient embryos, $Mis18\alpha^{\Delta/\Delta}$ MEFs showed mitotic defects, CENP-A loss in centromere and apoptotic cell death. Taken together, *Mis18α*-deficiency led the loss of CENP-A during cell division and hence missegregation of chromosome.

The 'licensing' role of Mis18α to load CENP-A to centromere without physical interaction supports the idea that CENP-A loading was managed by epigenetic regulation of centromere. Histone modifications, such as methylation or acetylation on lysine residues of histone H3, were reduced and transcripts from centromere region were increased in *Mis18α*$^{\Delta/\Delta}$ MEFs. Among enzymes regulating centromeric-histone modification and controlling transcripts from centromere, DNMT3A/3B interacted with Mis18α in leucine rich region (LRR) of Mis18α. The reduced localization of DNMT3A/3B to centromere in *Mis18α*$^{\Delta/\Delta}$ MEFs was rescued by Mis18α wildtype but not by Mis18α mutant possessing LRR mutation. Further, Mis18α and DNMT3A/3B mutually reinforced centromeric localization of each other. Bisulfite sequencing revealed that *Mis18α*-deficiency led to hypomethylation of DNA in centromere by reducing recruitment of DNMT3A/3B. Thus, 'licensing' function of Mis18α was obtained by interacting with DNMT3A/3B to maintain DNA methylation in centromere.

Taken together, CENP-A deposition during cell division was mediated through epigenetic regulation of centromeric DNA methylation by Mis18α/DNMT3A/3B complex. Epigenetic regulation of centromere by Mis18α to maintain CENP-A loading supports licensing function of Mis18α to retain centromeric identity.

Key words

Mis18α/ DNMT3A/ DNMT3B/ CENP-A/ Centromere/ Mitosis/ Chromosome segregation/ Histone modification/ DNA methylation/ Epigenetic regulation

CONTENTS

LIST OF FIGURES AND TABLES

CHAPTER I

Introduction

I-1 Centromere and CENP-A

1.1 Centromere

Centromere is a chromatin domain on which kinetochore, protein complex constructing platform linking each chromosome to mitotic spindle, assembled and which is necessary to mediate proper segregation of chromosome for delivery of genetic information to daughter cells (Amor et al., 2004; Cleveland et al., 2003). Centromere is composed of centromeric protein A (CENP-A) containing nucleosomes which is interspersed with canonical histone H3 containing nucleosome and centromeric DNA, alpha-satellite repeats (Yoda et al., 2000). Unlike histone H3, CENP-A is represented as a marker for centromere because CENP-A is only observed in centromere. Despite essential function of centromere in cell cycle, centromere structure is variable in different species. In yeast, centromere is relatively short region having repetitive consensus sequence of 125 base pairs on whole centromere (Henikoff et al., 2001). Otherwise, in human, centromere is composed of large repeat sequences, such as 0.3~5 megabases of alphoid DNA. Although centromeric DNA is prerequisite for identifying centromere in yeast, specific centromere can be formed on undetermined DNA sequences missing alpha-satellite repeats (Amor and Choo, 2002). This neocentromere found in human patient suggest that centromere is distinguished by CENP-A containing nucleosome rather than DNA sequence. Thus centromere identity is specified by epigenetic regulations.

1.2 Centromeric Proteins

Kinetochore is composed of constitutive centromeric proteins in inner and transient centromeric proteins in outer kinetochore. While transient centromeric proteins are in centromere at various cell cycle stages, essential constitutive centromeric proteins including CENP-A, CENP-B and CENP-C are present in centromere throughout the cell cycle (Sullivan et al., 1994). These proteins are required for the maintenance of centromere structure and the recruitment of other constitutive proteins and transient proteins responsible for spindle attachment (Cheeseman et al., 2002). CENP-A substituting histone H3 in centromeric nucleosome forms rigid heterotetramer with histone H4 by loop1 and α2 helix of the CENP-A histone fold domain (Black et al., 2004). *Cenp-a*$^{-/-}$ mice show severe damage in chromosome segregation including micro- and macronuclei formation, nuclear bridging and chromatin fragmentation and hence, lead to embryonic lethality in early stage (Howman et al., 2000). Although CENP-C is not a histone variant, it can interact with alpha-satellite domain of centromeric DNA but, not specifically (Politi et al., 2002). CENP-C is also fundamental component of centromere, supported by the results about embryonic lethality of *Cenp-c*$^{-/-}$ mice showing a missegregation phenotype and metaphase arrest (Fukagawa and Brown, 1997). CENP-B binds to 17 base pair motif, CENP-B box, in alpha-satellite DNA of centromere and participates in recruitment of other centromeric proteins (Sullivan and Glass, 1991). In comparison to other essential constitutive centromeric proteins, *Cenp-b*$^{-/-}$ mice are survive with decreased body weight, indicating that CENP-B is not essential for centromere

function (Perez-Castro et al., 1998).

1.3 CENP-A Deposition

Accurate segregation of chromosomes is achieved by maintenance of centromere, especially CENP-A assembly and propagation during cell division. Underlying mechanisms to be elucidated are how CENP-A specially deposited to centromere and when it happens. Recent studies revealed that deposition of newly synthesized CENP-A is occurred in specific cell cycle stages (Jansen et al., 2007). Fluorescent-based pulse-chase experiments demonstrated that CENP-A deposition to centromere is observed from telophase to early G1 phase unlike other histones observed in S-phase (Fig. IA). Further, DNA replication is not required for both deposition and mRNA or protein level of CENP-A, supporting that CENP-A deposition showed different pattern to canonical histones during cell cycle. However, the question about how pre-existing centromere is recognized by newly synthesized CENP-A is still unknown and therefore, CENP-A associated proteins are needed to be elucidated.

Centromeric proteins such as CENP-C, I and CENP-H are required for CENP-A deposition by recruitment of constitutive centromeric proteins (Okada et al., 2006). Complex purification of CENP-A reveals that HJURP (Holliday Junction Recognition Protein) is a component of CENP-A complex and required for CENP-A deposition in cell cycle dependent manner (Barnhart et al., 2011; Dunleavy et al., 2009; Shuaib et al., 2010). Knockdown of HJURP reduces CENP-A on centromere caused by impaired

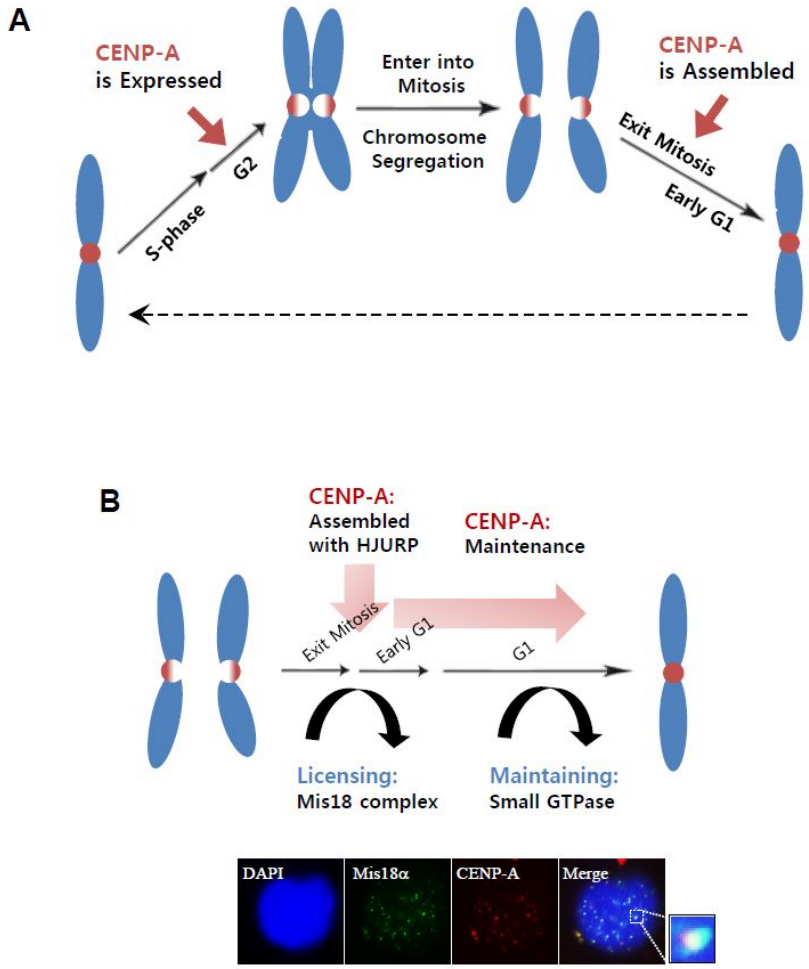

Figure I. Overview of CENP-A deposition

(A) A schematic diagram illustrating the CENP-A deposition during cell cycle. CENP-A protein is expressed at G2/M phase and then, incorporated into centromere from telophase to early G1 phase during mitosis. Images were adopted from Black et. al. (Black and Bassett, 2008). (B) The regulators responsible for CENP-A deposition during mitosis. Mis18 complex licenses newly synthesized CENP-A to load into centromere and then, newly incorporated CENP-A is maintained during G1 phase by GTPase activity. Bottom immunocytochemistry represents centromeric colocalization between Mis18α and CENP-A.

localization of newly synthesized CENP-A and hence, accumulates mitotic defects. Furthermore, the time window of centromeric localization of HJURP during cell cycle is identical to that of CENP-A. Therefore, HJURP is a molecular chaperone to perform exert CENP-A deposition on centromere.

Knockout based genetic screening in yeast has identified some of proteins required for CENP-A localization. In fission yeast, centromeric deposition of Cnp1 (human CENP-A) is reduced when Mis16 and Mis18 is disrupted (Hayashi et al., 2004). Further, RbAp46/48, human counter parts of Mis16, mediates CENP-A deposition and, reconstitute CENP-A containing nucleosomes in vitro in *Drosophila*. However, centromeric localization of these two molecules was not affected by absence of any of kinetochore proteins. These results implicate priming function of Mis16 and Mis18 for CENP-A loading (Fig. IB). Interestingly, Mis16 and Mis18 maintain deacetylated histone in centromere, suggesting that epigenetic regulation of centromere is important for CNEP-A deposition.

Recently, MgcRacGAP (a Rho family GTPase activating protein) is required to maintain newly incorporated CENP-A at the end of G1 phase by functional proteomics and high-resolution imaging (Lagana et al., 2010). MgcRacGAP is activator of Cdc42, one of the Rho family small GTPase, required for preservation of newly incorporated CENP-A. Cdc42 is recruited to centromere by KNL2, one of Mis18 complex, and cooperated with GTPase cycling to maintain newly incorporated CENP-A. Without GTPase activity, newly incorporated CENP-A was not distinguished to existed CENP-A and therefore, removed from centromrere during G1

phase. Taken together, a small GTPase switch ensures centromere function by maintenance of CENP-A on centromere after loading of CENP-A (Fig. IB). However, the question about how pre-existing centromere is recognized by newly synthesized CENP-A is still unknown.

I-2 Centromeric Chromatin States

2.1 Heterochromain States in Centromere

Centromere is composed of two distinct chromatin structure; CENP-A containing centric region and outside pericentric heterochromatin flanking centric region (Allshire and Karpen, 2008; Heit et al., 2011). Although centric and pericentric heterochromatins contain distinct characteristics, these regions share similar epigenetic marks, such as highly methylated DNA (Yamagata et al., 2007) and trimethylation on 9^{th} lysine residue of histone H3 (H3K9me3) (Guenatri et al., 2004). HP1 proteins are densely localized in pericentric heterochromatin region and also found in centric region (Craig et al., 2003). The heterochromatin is maintained by the cross-talk between DNA methyltransferases (DNMTs) including DNMT1 and DNMT3A/3B and histone modifying enzymes including SUV39H1 (Cedar and Bergman, 2009; Fuks et al., 2003; Lehnertz et al., 2003; Ling et al., 2004). In addition, RNAi machinery and noncoding transcripts from centromere regions are involved in proper formation of heterochromatin (Bouzinba-Segard et al., 2006; Grewal and Jia,

2007; Lippman and Martienssen, 2004; Verdel et al., 2004).

Centromere architecture is an important factor for centromere function as well as CENP-A loading (Black et al., 2007a; Bouzinba-Segard et al., 2006; Pidoux and Allshire, 2004). Accumulating evidences have shown that improper formation of centromere architecture causes defects in mitosis and CENP-A loading (Allshire et al., 1995; Santos et al., 2005; Yamagishi et al., 2008). In fission yeast, RNAi-mediated heterochromatin formation is critical for centromere formation and CENP-A loading, since the lack of H3K9 methyltransferase Clr4 or the ribonuclease Dicer abolishes establishing CENP-A chromatin (Folco et al., 2008). In a fungus *Neurospora crassa*, CENP-A distribution is altered either by mutation on an H3K9 methyltransferase *dim-5* or in the absence of HP1 (Smith et al., 2011). Misregulation of noncoding transcripts from minor satellite region has been shown to cause impaired mitosis and mislocalization of centromere associated proteins (Bouzinba-Segard et al., 2006). Deficiency of DNMT3A/3B leads to altered pericentric transcript level (Chen et al., 2004), and DNMT3B knockdown causes segregation defects (Gopalakrishnan et al., 2009).

2.2 Euchromatin States in Centromere

CENP-A nucleosomes in centromere are interrupted by histone H3 nucleosomes containing di-methylated Lys4 in H3 histone tails (Blower et al., 2002; Sullivan and Karpen, 2004). H3K4me2 is usually found in promoter region of expressed gene and represents marker for euchromatin region rather than

heterochromatin. The functional role of euchromatin states in centromere is elucidated by advantages of non-essential human artificial chromosome (HAC) acting like centromere (Bergmann et al., 2011; Nakano et al., 2008). Induced more open configuration in HAC by tetracyclin operator system cause missegregation of chromosome and loss of HAC. In addition, demethylation of H3K4me2 by LSD1, histone demethylase responsible for H3K4me2, lead reduced level of CENP-A and HJURP on HAC, suggesting that maintenance of H3K4me2-marked H3 nucleosome is crucial for CENP-A deposition. Furthermore, detection of transcripts from HAC supports these open chromatin structure within centromere. Despite euchromatin states including H3K4me2, centromeric euchromatin structure is not exactly matched to euchromatin in actively transcribed gene because another euchromatin marker including H3K9Ac and H3K4me3 is not found. Indeed, defects of centromere function mediated by induced open chromatin configuration are also observed in excessed heterochromatin states. Therefore, balanced maintenance between euchromatin and heterochromatin states is required for centromere function and supports epigenetic regulation of this function.

I-3 Mis18 Complex

3.1 Mis18α and Mis18β

Mis18 is identified as a regulator for CENP-A deposition in fission yeast (Hayashi et al., 2004). In human and mouse, there are two homologues for Mis18, designated Mis18α and Mis18β (Fujita et al., 2007). Complex purification of hMis18α in HeLa cells reveals interacting partners of hMis18α, such as Mis18β and other kinetochore proteins, RbAp46/48 and KNL2 (Mis18BP1). Although these proteins are responsible for CENP-A loading, those are not found in complex purification of CENP-A. As expected, hMis18α/ hMis18β/ hMis18BP1 localizes centromere and overlaps with CENP-A dot staining in nucleus. Interestingly, centromeric localization time window is from late anaphase to early G1 rather than localization of CENP-A through cell cycle and this time window is matched to that of newly synthesized CENP-A (Jansen et al., 2007). As in the results of spMis18 knockdown, missegregation of chromosomes and reduced centromeric localization of CENP-A and CENP-C is observed when any of hMis18 complex (hMis18α/ hMis18β/ hMis18BP1) is disrupted. Together, hMis18 complex has a 'priming' or 'licensing' role for deposition of newly synthesized CENP-A on centromere. Although TSA, histone deacetylase inhibitor, partly rescue CENP-A loss in knockdown of hMis18 complex, there are still unanswered questions about how hMis18 complex regulate centromeric chromatin without interaction with CENP-A and what activity hMis18

complex has for this regulation.

3.2 Mis18BP1

Mis18BP1 (KNL2) is larger protein (around 130 kDa) than the other components of Mis18 complex (around 30 kDa) and identified with various interacting partners. Direct binding between CENP-C and Mis18BP1 and, centromeric Mis18BP1 loss in depletion of CENP-C demonstrate that centromeric recruitment of Mis18 complex is mediated by CENP-C dependent centromeric localization (Moree et al., 2011). However, DNA binding activity of Mis18BP1 through myb-like DNA interacting domain also implicates the possibility that Mis18 complex can localize and bind to centromeric DNA during late mitosis (Maddox et al., 2007). In addition, in the maintenance of incorporated CENP-A in late G1 phase by small GTPase switch, centromeric localization of GTPase is mediated through interaction between Mis18BP1 and cdc42, one of the Rho family small GTPase (Lagana et al., 2010). This result expands licensing role of Mis18 complex to regulation of initiating maintenance mechanism about CENP-A loading.

CHAPTER II

Roles of Mis18α in Epigenetic Regulation of Centromeric Chromatin and CENP-A Loading

II-1. Summary

Centromeric protein A (CENP-A) deposition is critical steps to ensure proper segregation of chromosome during cell division. Although some proteins responsible for CENP-A deposition have been identified, physiological role and its significance in development are not elucidated yet. Mis18 complex has been identified as a critical factor for the centromeric localization of CENP-A, which is responsible for the specification of centromere identity in the chromosome. However, the functional role of Mis18 complex is largely unknown. Here, I characterized *Mis18α* conditional knockout mice and found that *Mis18α*-deficiency resulted in lethality at early embryonic stage with severe defects in chromosome segregation caused by mislocalization of CENP-A. Similar to *Mis18α*-deficient embryos, *Mis18α*$^{\Delta/\Delta}$ MEFs exhibited CNEP-A loss and mitotic abnormality. These chromosomal defects led to accumulate DNA damage and genomic instability, and hence led to apoptotic cell death. Further, Mis18α's crucial role for epigenetic regulation of centromeric chromatin was demonstrated by reinforcing centromeric localization of DNMT3A/3B using *Mis18α*-deficient MEFs. Mis18α interacts with DNMT3A/3B through its C-terminal leucine rich region and this interaction is critical for maintaining DNA methylation and hence regulating epigenetic states of centromeric chromatin. *Mis18α*-deficiency led to reduced DNA methylation, altered histone modifications, and uncontrolled noncoding

transcripts in centromere region by decreased DNMT3A/3B enrichment. Therefore, centromeric localization of CENP-A during mitosis was preserved by Mis18α mediated centromeric-chromatin states. Together, these findings uncover the functional mechanism of Mis18α and its pivotal role in mammalian cell cycle.

II-2. Introduction

Centromere is required for accurate segregation of chromosome by serving as a platform to form a kinetochore, a macromolecular protein structure linking each chromosome to mitotic spindle (Cleveland et al., 2003; Pidoux and Allshire, 2000; Sullivan et al., 2001; Kline-Smith et al., 2005). In budding yeast, the location of centromere is determined by DNA sequences which recruit sequence-specific DNA binding proteins (Fitzgerald-Hayes et al., 1982), while in higher eukaryotes, centromere region is determined epigenetically by the incorporation of histone H3 variant, CENP-A (Allshire and Karpen, 2008; Bernad et al., 2009; Palmer et al., 1991; Sullivan et al., 1994). CENP-A identifies and forms centromere by its unique centromere targeting domain (CATD) which is not in other histones (Foltz et al., 2006; Sekulic et al., 2010). CENP-A forms nucleosomes with canonical histones, H2A, H2B, and H4 at the active centromeres, and CENP-A containing nucleosomes are recognized by other centromeric components such as CENP-N and CENP-C referred to as CCAN (constitutive centromere associated network) to form a higher order structure (Carroll et al., 2010; Carroll et al., 2009; Foltz et al., 2006). Centromere proteins belonging to kinetochore are required for formation of kinetochore as a building block and for functional roles of centromere as constitutive or transient regulators (Ando et al., 2002; Black et al., 2004). CENP-A and its complex including CENP-B and CENP-C are required for the recruitment of constitutive centromere proteins and transient

centromere proteins mediating microtubule attachment. *Cenp-a* knockout mice was lethal and showed severe defects in mitosis including nuclear bridges, and chromatin fragmentation (Howman et al., 2000). *Cenp-c* knockout mice are also lethal in early embryonic stages which is slightly earlier than the time when *Cenp-a* knockout mice died (Kalitsis et al., 1998). While *Cenp-a* and *Cenp-c* knockout mice are early embryonic lethal, *cenp-b* knockout mice was survive and grow normal, indicating that Cenp-b is not essential for structure and function of centromere (Hudson et al., 1998).

The centromere region possesses heterochromatic characteristics such as tri-methylation on 9th lysine residue of histone H3 (H3K9me3) (Guenatri et al., 2004; Martens et al., 2005), localization of HP1 proteins in metaphase (Craig et al., 2003; Gopalakrishnan et al., 2009) and highly methylated DNA (Chen et al., 2003; Yamagata et al., 2007). RNAi machinery and noncoding transcripts from centromere region for heterochromatin maintenance are also involved in centromere architecture and function (Bouzinba-Segard et al., 2006; Grewal and Jia, 2007; Lippman and Martienssen, 2004; Verdel et al., 2004). In addition, deficiency of DNMT3A/3B leads to altered centromeric transcript level, and DNMT3B knockdown causes chromosome segregation defects (Chen et al., 2004). On the other hand, euchromatic states are also found in centromere region. CENP-A nucleosomes in centromere are interspersed with H3K4me2 containing nucleosomes (Bergmann et al., 2011). This open chromatin state is crucial for kinetochore function.

The mechanisms of how newly synthesized CENP-A are deposited to and maintained in the centromere have long been unanswered. Recent studies gave a clue

for this question by identifying several new players in this process. HJURP (holiday junction recognizing protein) has been identified as a CENP-A-specific chaperone, which directly interacts with newly synthesized CENP-A through the centromere targeting domain (CATD) of CENP-A and guides CENP-A for its deposition into the centromeric nucleosomes (Bernad et al., 2011; Black et al., 2007b; Dunleavy et al., 2009; Foltz et al., 2009; Pidoux et al., 2009; Shuaib et al., 2010). Mis18 in fission yeast and Mis18 complex (Mis18α, Mis18β, and Mis18BP1/HsKNL2) in higher eukaryotes also play a critical role in centromere localization of CENP-A (Fujita et al., 2007; Hayashi et al., 2004; Maddox et al., 2007). Mis18 complex accumulates at the centromere during anaphase to early G1 phase of cell cycle, which is slightly ahead of CENP-A loading, and its knockdown causes mislocalization of CENP-A, suggesting its "licensing or priming function" for centromeric localization of newly synthesized CENP-A (Fujita et al., 2007; Silva and Jansen, 2009). However, unlike HJURP, Mis18 complex does not directly interact with CENP-A (Fujita et al., 2007; Hayashi et al., 2004). Recently, it was reported that Mis18 complex is required for HJURP localization to centromere (Barnhart et al., 2011), but it is still unknown how Mis18 complex mediates HJURP without physically interacting with HJURP/CENP-A complex (Shuaib et al., 2010). In addition to these proteins, a Rho family small GTPase complex containing MgcRacGAP, ECT2, and Cdc42 (or Rac) has been shown to be a maintenance factor for newly incorporated CENP-A at centromeres (Lagana et al., 2010). This GTPase localizes to the centromere at late G1 phase, showing its

distinct role from licensing or loading factors.

In the present study, functional roles of Mis18 were verified in embryonic development through generation of *Mis18α*$^{\Delta/\Delta}$ mice. CENP-A loss and chromosome missegregation in *Mis18α*$^{\Delta/\Delta}$ embryos led early embryonic lethality by apoptotic cell death. This phenotype was confirmed in *Mis18α*$^{\Delta/\Delta}$ MEFs, suggesting that accumulation of mitotic defects mediated by CENP-A loss is the cause of embryonic death of *Mis18α*$^{\Delta/\Delta}$ mice. Further, altered histone modification patterns and concomitantly increased noncoding transcripts at centromere region in *Mis18α*-deleted mouse embryonic fibroblast (MEF) was identified. DNMT3A/3B as interacting partners of Mis18α and their interaction turned out to be crucial for maintaining methylation status of centromeric DNA and licensing CENP-A loading. Together, these data strongly demonstrate that Mis18α reinforces centromere localization of DNMT3A/3B to ensure proper epigenetic states of centromeric chromatin so that newly synthesized CENP-A can be properly located to centromere.

II-3. Results

Generation of Mis18α knockout mouse

To elucidate physiological roles of Mis18 *in vivo*, *Mis18α* conditional knockout mice, in which exons 1 and 2 of the *Mis18α* gene is flanked by *loxP* sites so that ATG start codon can be deleted was generated (Fig. II-1A). The *loxP* flanked Neo cassette from a pGK-gb2 loxP/FRT-Neo was inserted on the 3' side of exon 2 and the single loxP site is inserted at the 5' side of exon 1. After selection in G418 antibiotic, surviving clones were expanded to identify recombinant ES clones by Southern blot analysis. For *Eco*RI digestion, the bands representing wild-type and mutant alleles are 8.4 and 6.6 kb, respectively (Fig. II-1B). Resulting mice harboring an allele of deleted exons 1 and 2 of *Mis18α* gene was designated to $Mis18\alpha^{+/\Delta}$. The heterozygous $Mis18\alpha^{+/\Delta}$ mice were phenotypically normal without any obvious impairment of growth and fertility. However, when they were intercrossed, no homozygous *Mis18α* deleted mouse ($Mis18\alpha^{\Delta/\Delta}$) was detected (Fig. II-1C). No alive embryo was detected at either embryonic days 12.5 (E12.5) or E9.5 from heterozygote mating, indicating that inactivation of both alleles leads to early embryonic lethality.

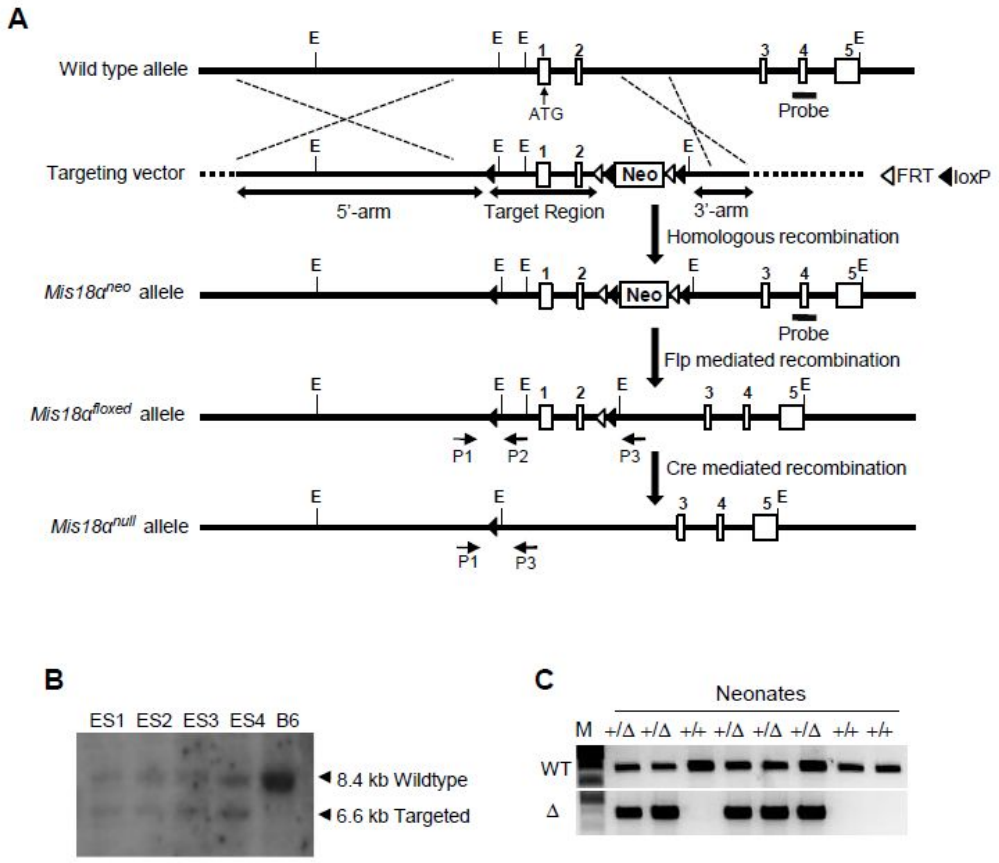

Figure II-1. Generation of *Mis18α*$^{-/-}$ mice

(A) A schematic diagram of producing a conditional *Mis18α* knockout mouse. Exons 1 and 2 were flanked by *loxP* sequences. (B) Southern Screening to identify recombinant ES (embryonic stem) cell clones. (C) Representative genotyping result for neonates. An allele with deleted exons 1 and 2 was designated to Δ.

Mis18α Deficiency Caused Lethality during Early Embryogenesis

Based on the early embryonic lethality of *Cenp-a* knockout mice (Howman et al., 2000), E3.5 embryos prepared. All embryos were morphologically normal in visual inspection using microscope (Fig. II-2A). After genotyped all embryos, 20 *Mis18α*$^{\Delta/\Delta}$ embryos among 67 total embryos were identified, indicating that *Mis18α*$^{\Delta/\Delta}$ embryos are alive at least until E3.5 (Fig. II-2B). To further define the timing of embryonic lethality, E7.5 embryos were analyzed and genotyped. *Mis18α*$^{\Delta/\Delta}$ embryos were not passed through embryogenesis from E3.5 to E7.5 (Fig. II-2C and 2D). Therefore, *Mis18α*$^{\Delta/\Delta}$ embryos showed defective development after E3.5 and serially degraded until E7.5 (Fig. II-2E). To verify stages of defective embryogenesis in *Mis18α*$^{\Delta/\Delta}$ embryo, embryos from heterozygote mating were flushed at E3.5 and then inspected for *in vitro* growth for another 4 days. In *Mis18α*$^{+/+}$ or *Mis18α*$^{+/\Delta}$ genotypes, embryos hatched and formed inner cell mass and trophoblasts on 48 hr of culture. The inner cell mass became apparent on 72 hr and grew normally for at least 96 hr after embryo culture (Fig. II-3A, upper 4 lines). *Mis18α*$^{\Delta/\Delta}$ embryos hatched normally, however, inner cell mass did not grow well and formed only small mass compared to that of *Mis18α*$^{+/+}$ or *Mis18α*$^{+/\Delta}$ on 72 hr of culture. These embryos finally degenerated and cell mass was no longer visible on the fourth day of culture (Fig. II-3B, bottom 2 lines). Taken together, *Mis18α*-deficient mice are lethal in early embryonic stage, indicating indispensable role of Mis18α in embryogenesis.

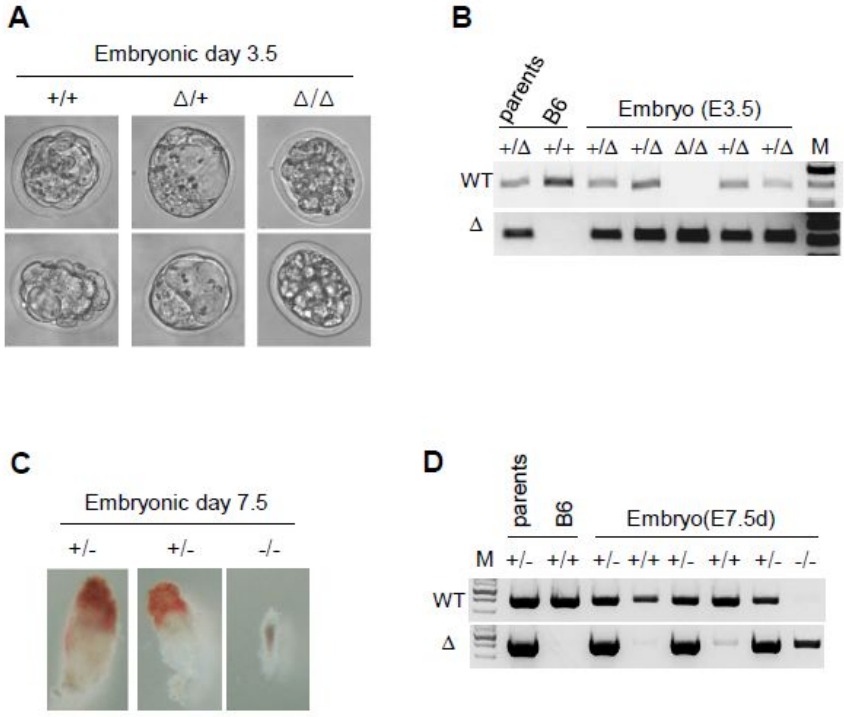

E

Embryonic Day	No. and (%) of embryos by genotype			Total
	+/+	+/Δ	Δ/Δ	
neonates	26 (33)	55 (70)	0 (0)	79
12.5	10 (29)	25 (71)	0 (0)	35
9.5	4 (17)	19 (83)	0 (0)	23
3.5	15 (22)	32 (48)	20 (30)	67

Figure II-2. Early embryonic lethality of Mis18α-deficient mice

(A) *Mis18α* knockout embryos was survived in blastocyst stages. (B) Representative genotyping result for E3.5 embryos. An allele with deleted exons 1 and 2 was designated to Δ. (C) Impaired growth of *Mis18α* knockout embryos in early embryonic development. (D) Representative genotyping result for E7.5 embryos. (E) Summary of genotyping results for neonates and embryos. The numbers in parentheses refer to the percentage of each genotype per total embryos.

A

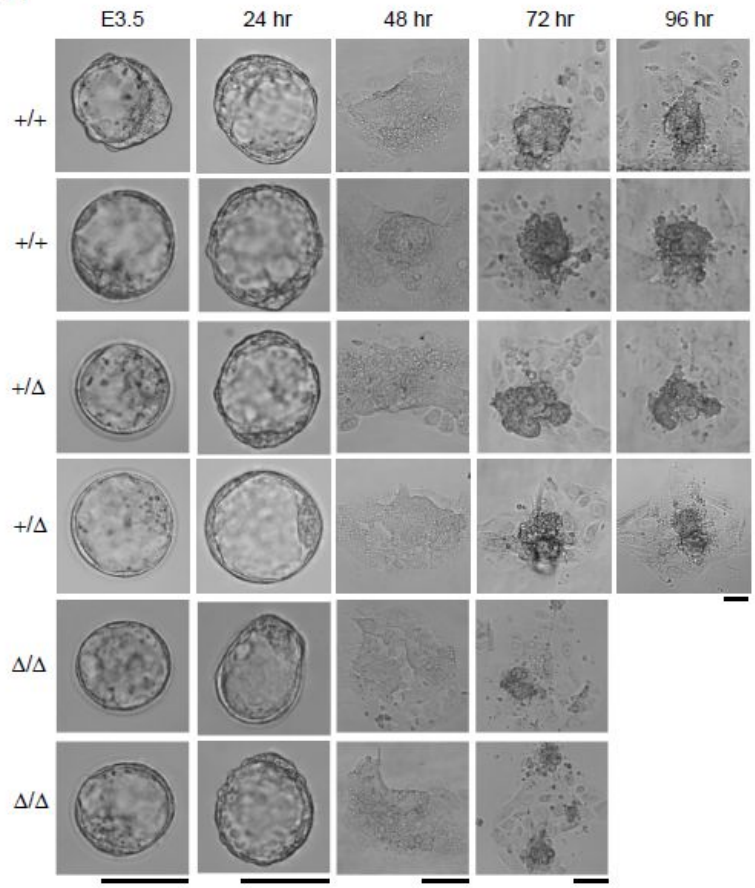

B

Embryonic Day	No. and (%) of embryos by genotype			Total
	+/+	+/Δ	Δ/Δ	
outgrowth	6 (33)	5 (28)	7 (39)	18

Figure II-3. Defective growth of inner cell mass in Mis18α-deficient embyos
(A) Blastocysts outgrowth. Embryos from heterozygote intercross were flushed at E3.5 and cultured *in vitro* in ES cell medium. All scale bars represent 100 μm. (B) Summary of genotyping results for outgrowth analysis. The numbers in parentheses refer to the percentage of each genotype per total embryos.

***Mis18α* Deficiency Causes Severe Chromosomal Missegregation Leading to Cell Death**

To gain insight into the cause of death of *Mis18α*$^{\Delta/\Delta}$ embryos, the mitotic progression of cultured embryos at E4.5 were examined by immunofluorescence analysis. The mitotic stage of cells was visualized by the phosphorylation of H3S10 and microtubule-attachment to chromosomes was examined by staining α-tubulin. Unlike *Mis18α*$^{+/+}$ embryos (Fig. II-4A, a-b), mitotic defects such as misaligned chromosomes and microtubules were frequently observed in high resolution images for *Mis18α*$^{\Delta/\Delta}$ embryos (~85% cells in mitotic stages, Fig. II-4A, c-d). *Mis18α*$^{+/+}$ cells showed a straight alignment of chromosomes to the equator and normal bipolar orientation of spindle microtubules (Fig. II-4B, left panel). In contrast, *Mis18α*$^{\Delta/\Delta}$ cells exhibited misalignment of chromosomes as well as satellite chromosomes (Fig. II-4B, right panel and solid triangle). In addition, *Mis18α*$^{\Delta/\Delta}$ cells displayed improper microtubule attachment to chromosomes (Fig. II-4B, open triangle), inappropriate chromosome congression in prometaphase, anaphase bridges, and lagging chromosomes in telophase resulting in fragmented chromosomes (Fig. II-4C). These results suggest Mis18α is crucial for the chromosome segregation in embryonic cells.

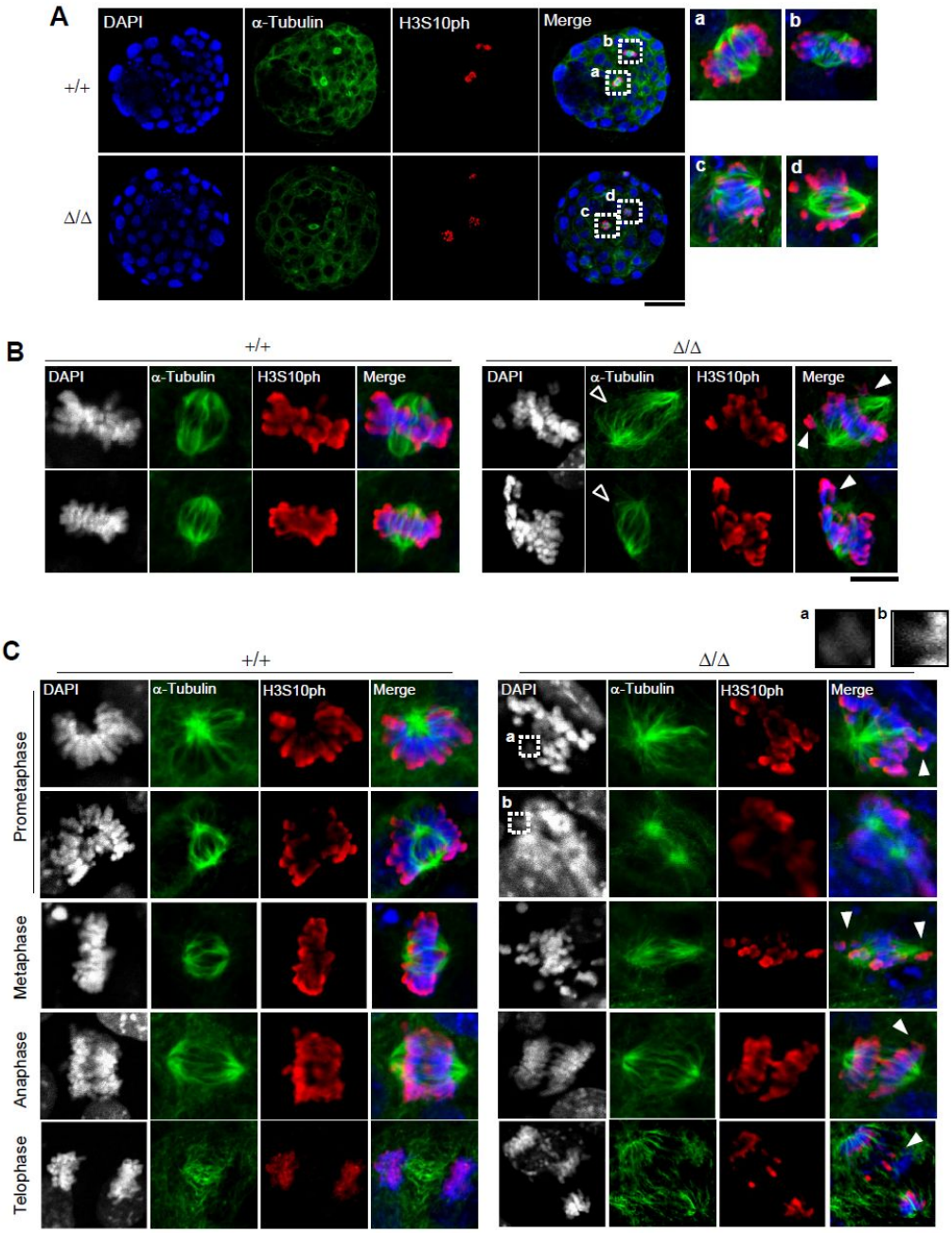
A
DAPI
α-Tubulin
H3S10ph
Merge
+/+
Δ/Δ
a
b
c
d
B
+/+
Δ/Δ
DAPI
α-Tubulin
H3S10ph
Merge
C
+/+
Δ/Δ
Prometaphase
Metaphase
Anaphase
Telophase

Figure II-4. Mitotic defects in *Mis18α*$^{\Delta/\Delta}$ embryos

(A) Immunocytochemistry of *Mis18α*$^{+/+}$ and *Mis18α*$^{\Delta/\Delta}$ embryos (E4.5). Antibodies against phospho-H3S10 (red) and α-tubulin (green) were used to visualize mitotic stage cells and microtubules, respectively. Nuclei were stained with DAPI (blue). The insets (a - d) in merged images are magnified to the right side. Scale bar: 40 μm. (B) Mitotic cell images showing that *Mis18α*$^{\Delta/\Delta}$ embryos (E4.5) are possessing missegregation of chromosomes while *Mis18α*$^{+/+}$ embryos are not. Antibodies against phospho-H3S10 (red) and α-tubulin (green) were used. Nuclei were stained with DAPI (blue). The insets (a and b) in images are magnified to the upper right side. Missegregated or satellite chromosomes (closed arrows) are indicated in *Mis18α*$^{\Delta/\Delta}$ embryonic cells. The scale bar: 10 μm.

Knockdown of Mis18α in HeLa cells has been shown to abrogate proper loading of newly synthesized CENP-A to centromere, and producing defects in chromosome segregation (Fujita et al., 2007). Since chromosomal missegregation was found in *Mis18α*$^{\Delta/\Delta}$ blastocysts, it was questioned whether it is from CENP-A loading problem as shown in HeLa cells. Unlike clear dot shaped nuclear CENP-A in the most of DAPI positive cells in *Mis18α*$^{+/+}$ embryos, the number of cells showing nuclear CENP-A were significantly reduced in *Mis18α*$^{\Delta/\Delta}$ embryos (Fig. II-5A). While less than 10% of *Mis18α*$^{+/+}$ cells failed to show CENP-A dots, over 65% of *Mis18α*-deficient cells showed aberrant CENP-A dots (Fig. II-5B). Lack of CENP-A dot indicates loss of basic building block of centromere, which leads to inaccurate attachment of kinetochore to the centromere and missegregation of chromosome during cell division. Therefore, cell death in *Mis18α*$^{\Delta/\Delta}$ embryos might be due to the accumulated mitotic defects during cell division processes. To prove this hypothesis, TUNEL assay was performed on cultured E5.0 embryos. *Mis18α*$^{\Delta/\Delta}$ embryos exhibited a statistically higher percentage of TUNEL positive cells (7.8 ± 1.5 per embryo) than did *Mis18α*$^{+/+}$ embryos (1.8 ± 0.3 per embryo) (Fig. II-6A and II-6B). Taken together, *Mis18α*-deficiency caused defect in centromeric localization of CENP-A, which in turn resulted in the missegregation of chromosomes during embryonic cell division and eventually, cell death. The accumulation of dead cells led to early lethality of *Mis18α*$^{\Delta/\Delta}$ embryos, suggesting that Mis18α is a pivotal component for the progression of embryonic development.

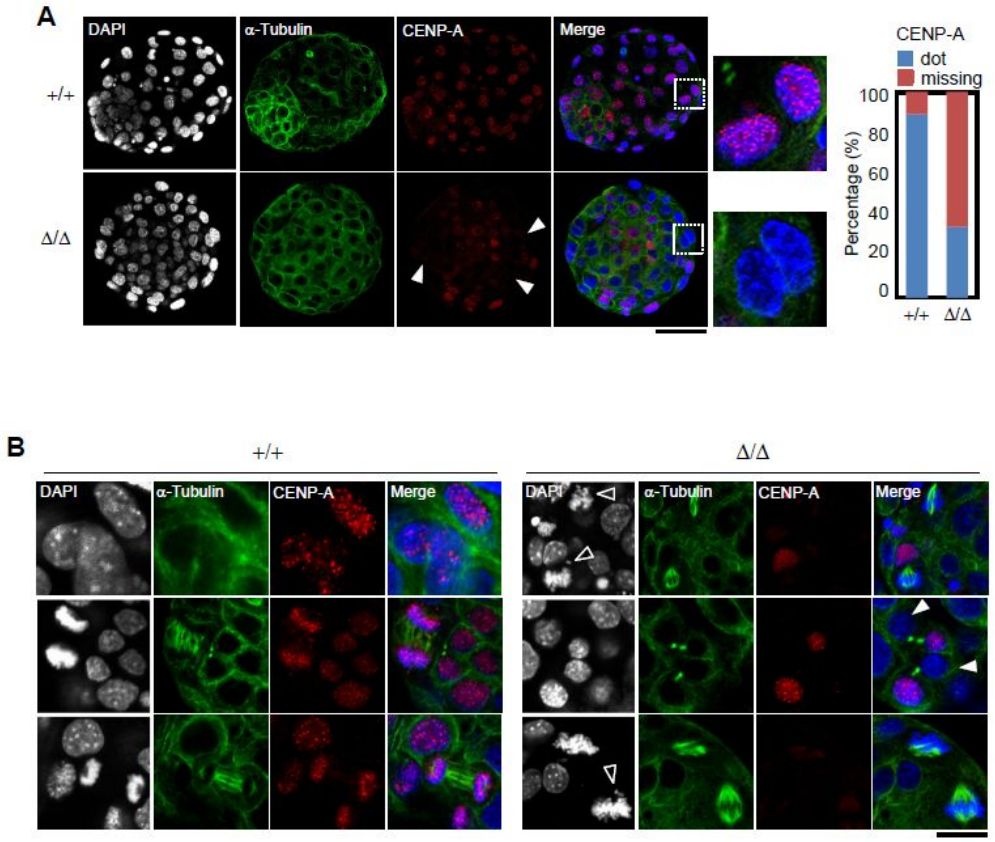

Figure II-5. CENP-A loss in *Mis18α*$^{\Delta/\Delta}$ embryos

(A) Representative images to show CENP-A in *Mis18α*$^{+/+}$ and *Mis18α*$^{\Delta/\Delta}$ embryos (E4.5). Closed arrows indicate lacking of CENP-A dots. The histogram on the right shows percentage of cells exhibiting CENP-A dot signal. These are mean values from counting 10 embryos each. Scale bar: 40 μm. (B) Representative images showing CENP-A loss during mitosis in *Mis18α*$^{+/+}$ and *Mis18α*$^{\Delta/\Delta}$ embryos (E4.5). Satellite chromosomes (open arrow) or loss of CENP-A dots (closed arrow) were indicated in *Mis18α*$^{\Delta/\Delta}$ embryonic cells. Scale bar: 20 μm.

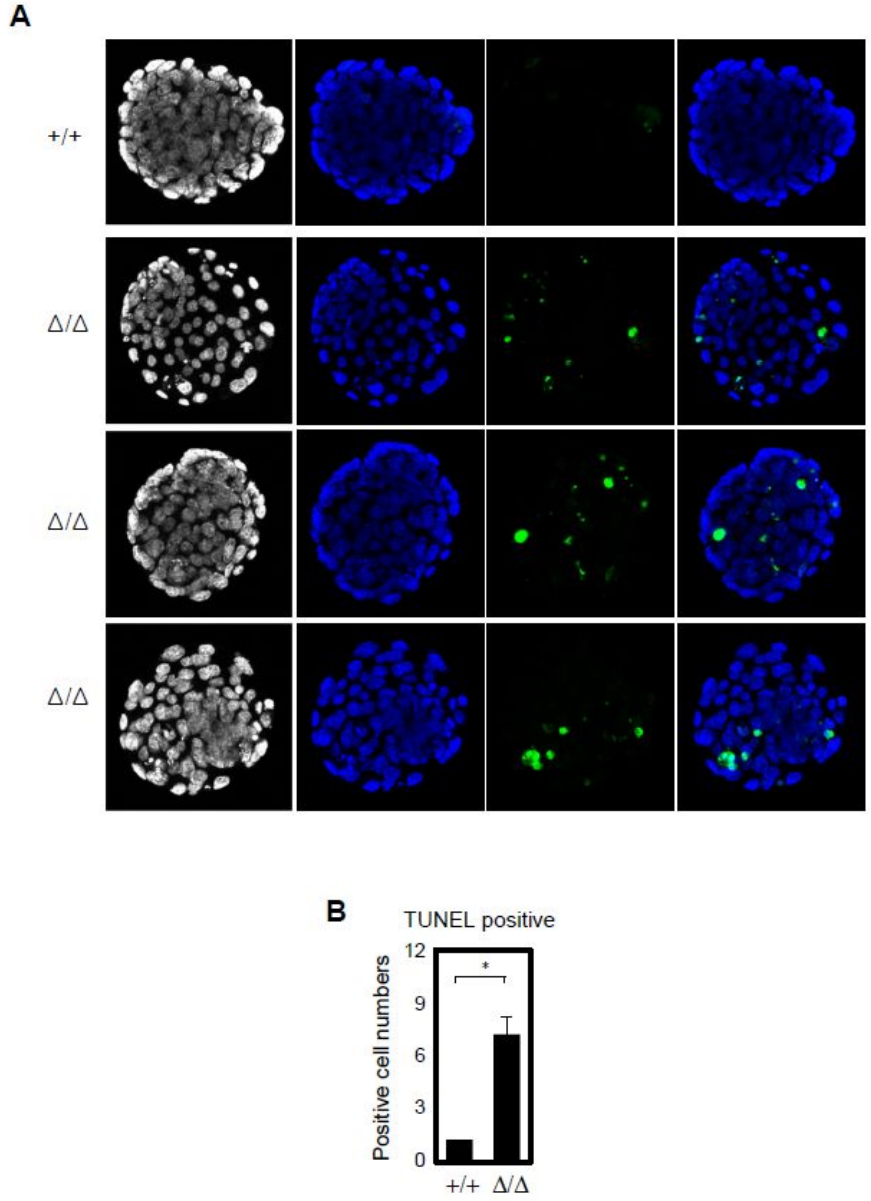

Figure II-6. Apoptotic cell death in Mis18α-deficient embryos

(A) TUNEL assay in E5.0 embryos. TUNEL positive cells were stained green and DAPI (blue) was for nuclei. P-value is calculated by t-test (∗ : $p < 0.05$). Scale bar: 40 μm. (B) Histogram represents the percentage of TUNEL positive cells per embryo from counting of 10 embryos per each group.

The Defects of Chromosome Segregation and Centromere Organization in *Mis18α*-deficient Fibroblast

MEFs harboring *Mis18α*$^{+/\Delta}$ or *Mis18α*$^{f/\Delta}$ (*f* for floxed) genotypes were generated since *Mis18α*$^{\Delta/\Delta}$ MEFs were not able to be generated due to embryonic lethality. In *Mis18α*$^{f/\Delta}$ MEFs, endogenous Mis18α gradually decreased after Cre-expression and was no longer detectable from day 7 whereas no significant change was seen in *Mis18α*$^{+/\Delta}$ MEFs (Fig. II-7A). The total amount of CENP-A in *Mis18α*$^{+/\Delta}$ or *Mis18α*$^{f/\Delta}$ MEFs before and after cre-expression was not changed as shown by immunoblot. Hereafter, the term *Mis18α*$^{\Delta/\Delta}$ MEFs was used for the Cre-expressing *Mis18α*$^{f/\Delta}$ MEFs at day 5 or 7, as endogenous Mis18α was barely detectable. Since *Mis18α*$^{\Delta/\Delta}$ cells in blastocysts showed growth defect, the growth property of MEF cells was first checked. Unlike *Mis18α*$^{+/\Delta}$ and *Mis18α*$^{f/\Delta}$ MEFs showing normal growth properties, Cre-expressing *Mis18α*$^{f/\Delta}$ (*Mis18α*$^{\Delta/\Delta}$) MEFs showed severe growth retardation from day 4, indicating crucial role of Mis18α for cell growth (Fig. II-7B). Indeed, morphological abnormality of nuclei was found in *Mis18α*$^{\Delta/\Delta}$ MEFs using DAPI staining. Mis18α-deficient cells showed grape-shaped or fragmented nuclei which were usually found in abnormal cells having missegregation (Fig. II-7C).

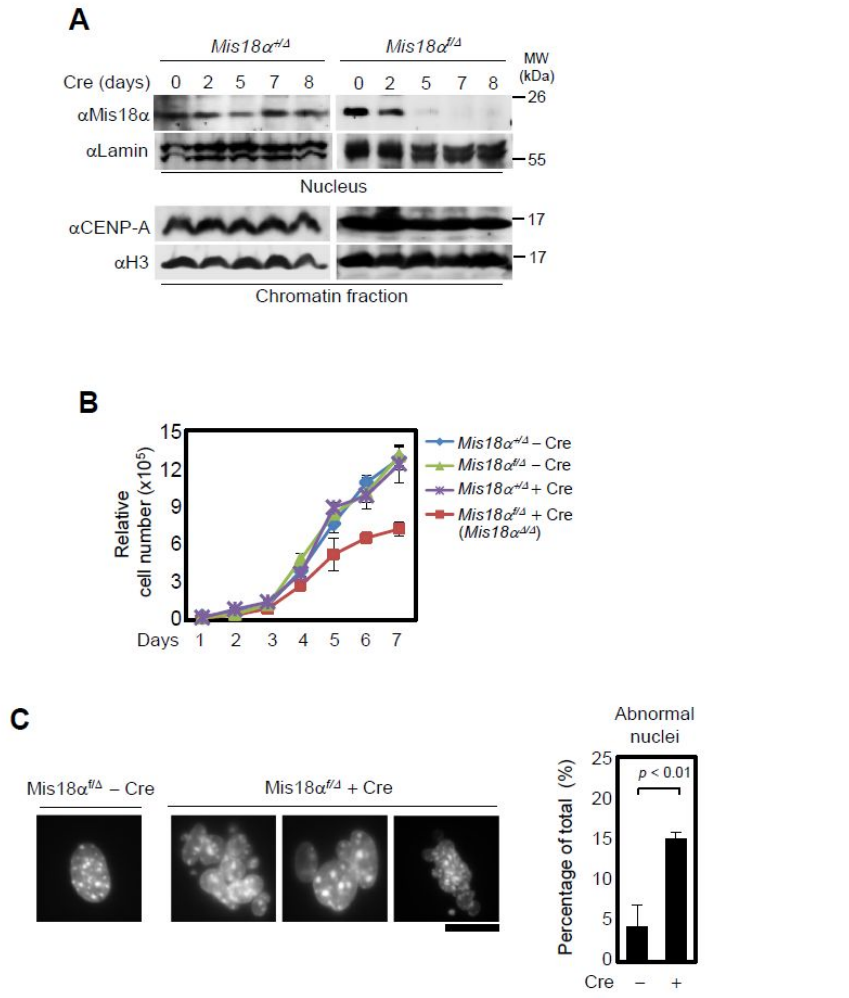

Figure II-7. Growth defects in Mis18α-deficient embryonic fibroblast cells

(A) Endogenous Mis18α in MEFs after Cre-expressing retroviral infection. Nuclear extracts from *Mis18α*$^{+/\Delta}$ and *Mis18α*$^{f/\Delta}$ were used for immunoblot analysis. Lamin was used as a loading control. For indicating total amount of CENP-A, chromatin fraction was prepared and histone H3 was used as a loading control. (B) Growth properties of *Mis18α*$^{+/\Delta}$ and *Mis18α*$^{f/\Delta}$ MEFs with or without Cre-expression. One day after Cre-expression, each group consisting of 1 x 10^4 cells was seeded and cultured for another 7 days. The values are expressed as mean ± SEM of three independent experiments. (C) Abnormal nuclei were found in *Mis18α*$^{f/\Delta}$ MEFs with Cre-infection. Right side histogram represents the percentage of abnormal nuclei of total 400 cells.

Next, immunocytochemistry was performed to compare mitotic stages of *Mis18α*$^{+/\Delta}$ to *Mis18α*$^{f/\Delta}$ MEFs. Similar to *Mis18α*$^{\Delta/\Delta}$ cells in blastocysts, about 60 % of Mis18α-deficient MEFs exhibited chromosomal bridge in anaphase, or lagging chromosome in telophase (Fig. II-8A, closed arrow). Furthermore, about 50 % of *Mis18α*$^{\Delta/\Delta}$ MEFs failed to show centromeric CENP-A dots compared to *Mis18α*$^{f/\Delta}$ MEFs in interphase stage (Fig. II-8B), as *Mis18α*$^{\Delta/\Delta}$ cells in blastocysts showed (Fig. II-4B). To further analysis of mitotic stage cells, spreading assay using *Mis18α*$^{+/\Delta}$ to *Mis18α*$^{f/\Delta}$ MEFs was performed metaphase. First, arrangement and morphology of metaphase chromosomes were compared between them. As expected, satellite chromosomes and decondensed shape of chromosomes were found in *Mis18α*$^{\Delta/\Delta}$ MEFs (Fig. II-9A). Then, relationship between CENP-A localization and abnormal chromosome were tested using immunocytochemistry. While almost all *Mis18α*$^{+/\Delta}$ MEFs show positive CENP-A staining and organized chromosomes, *Mis18α*$^{\Delta/\Delta}$ MEFs exhibited several abnormal phenotypes related to chromosome segregation including defective chromosome condensation in prometaphase and CENP-A loss in about 50 % of total cells (Fig. II-9B, box images a and b). Taken together, *Mis18α*$^{\Delta/\Delta}$ MEFs have the same defects in chromosome segregation as shown in *Mis18α*$^{\Delta/\Delta}$ blastocysts and CENP-A loss in *Mis18α*$^{\Delta/\Delta}$ MEFs is causal defect in mitotic abnormality.

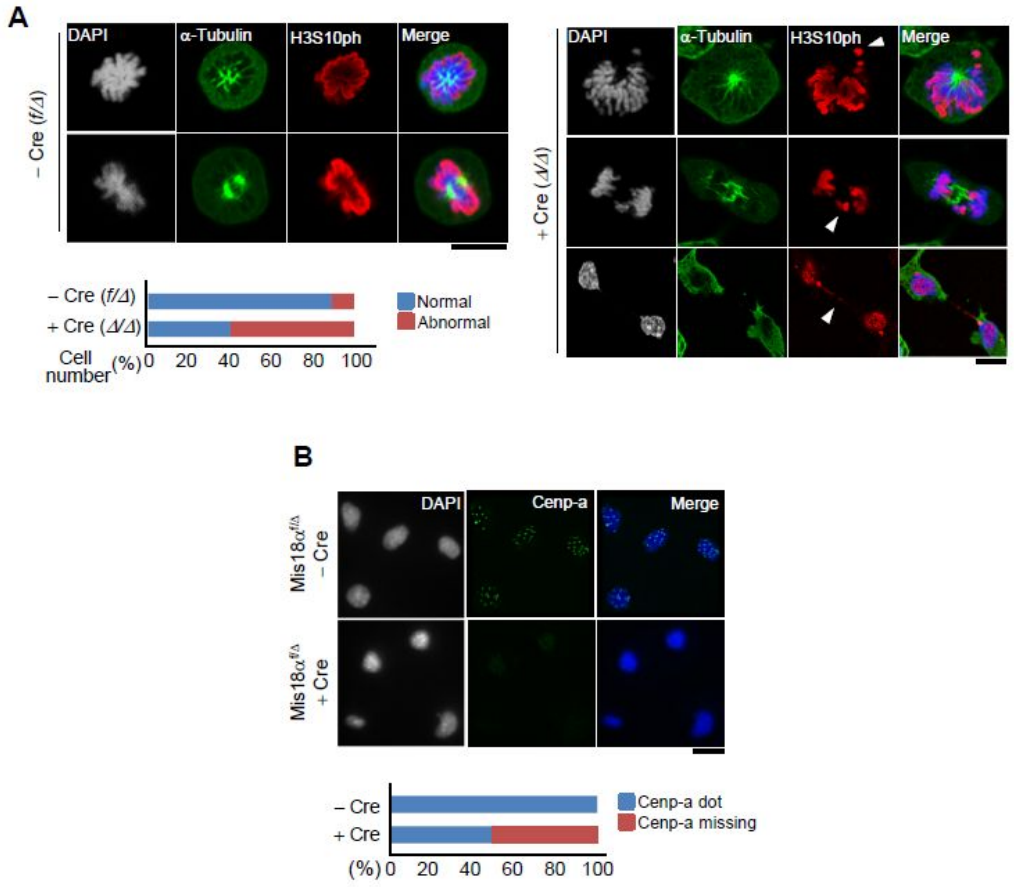

Figure II-8. Mitotic defects and CENP-A loss in Mis18α-deficient MEFs

(A) *Mis18α*$^{f/\Delta}$ and *Mis18α*$^{\Delta/\Delta}$ MEFs were applied for the immunocytochemistry with antibodies against phospho-H3S10 (red) or α-tubulin (green). Histogram shows percentage of 50 mitotic cells exhibiting normal chromosomes versus abnormal chromosomes. Scale bars: 10 μm. (B) Immunocytochemistry was performed in *Mis18α*$^{f/\Delta}$ and *Mis18α*$^{\Delta/\Delta}$ MEFs. The percentage of cells showing CENP-A dots (red) was calculated by counting 400 cells. DAPI (blue) was used to stain nucleus.

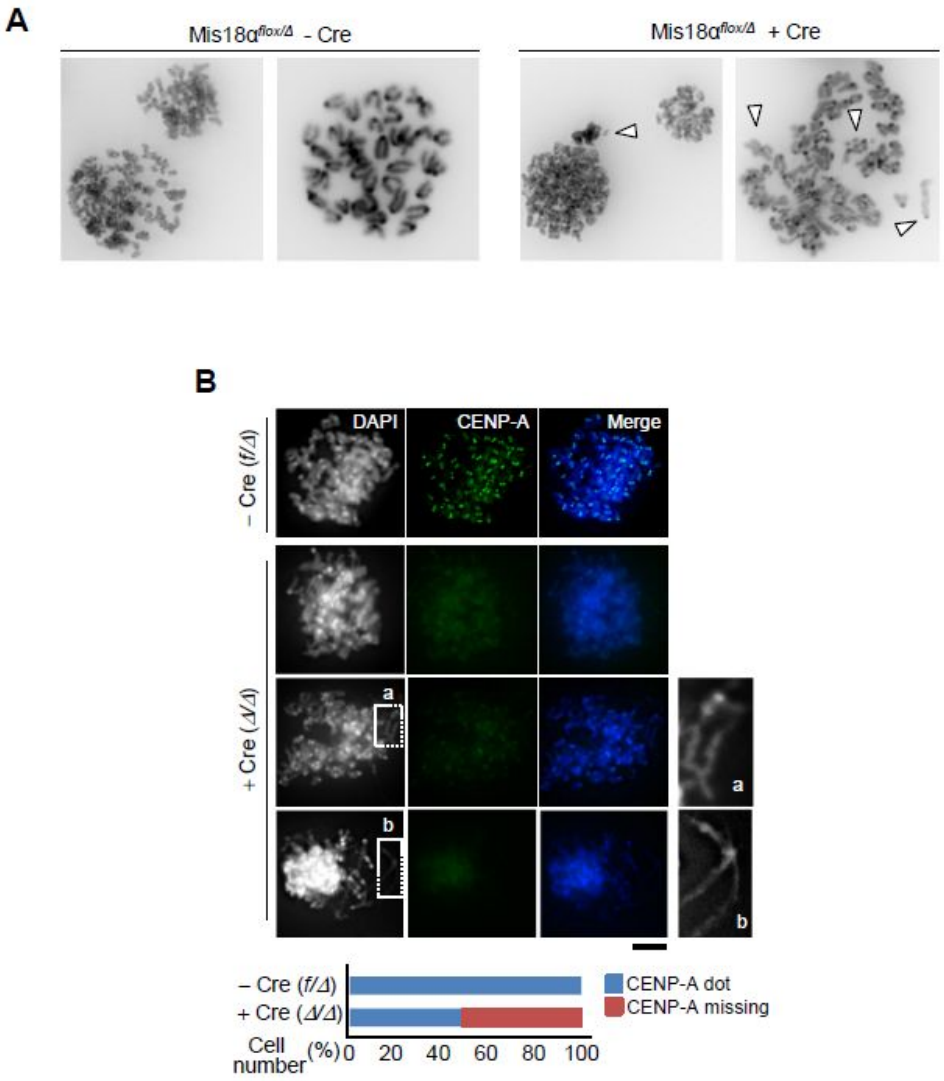

Figure II-9. Chromosomal defects of Mis18α-deficient MEFs

(A) Chromosome spreading assay in *Mis18α*$^{f/\Delta}$ (–Cre) and *Mis18α*$^{\Delta/\Delta}$ (+Cre) MEFs. Satellite chromosomes or decondensed chromosomes were indicated by open arrow. (B) Mitotic chromosome was spread from *Mis18α*$^{f/\Delta}$ (–Cre) and *Mis18α*$^{\Delta/\Delta}$ (+Cre) MEFs, and stained using antibody against CENP-A (green). Histogram shows percentage of cells exhibiting CENP-A dots, which is generated from counting 200 cells. The insets (a and b) are magnified to the right side. Scale bar: 10 μm.

Mis18α-deficient MEFs Show Apoptotic Cell Death

To verify whether accumulation of mitotic defects mediates cell death in *Mis18α*$^{\Delta/\Delta}$ MEFs as in *Mis18α*$^{\Delta/\Delta}$ blastocysts, TUNEL assay was performed. *Mis18α*$^{\Delta/\Delta}$ MEFs exhibited a statistically higher percentage of TUNEL positive cells (25 ± 4 % of total cells) than did *Mis18α*$^{+/+}$ embryos (4 ± 1 % of total cells) (Fig. II-10A). Furthermore, DNA damage, such as DNA double strand break, was occurred in *Mis18α*$^{\Delta/\Delta}$ MEFs using γH2AX staining (Fig. II-10B). Therefore, CENP-A loss and mitotic defects by *Mis18α*-deficiency caused cell death in MEFs and early embryonic cells. Taken together, Mis18α has a pivotal role in cell cycle progression by regulation of CENP-A localization and proper segregation during cell division.

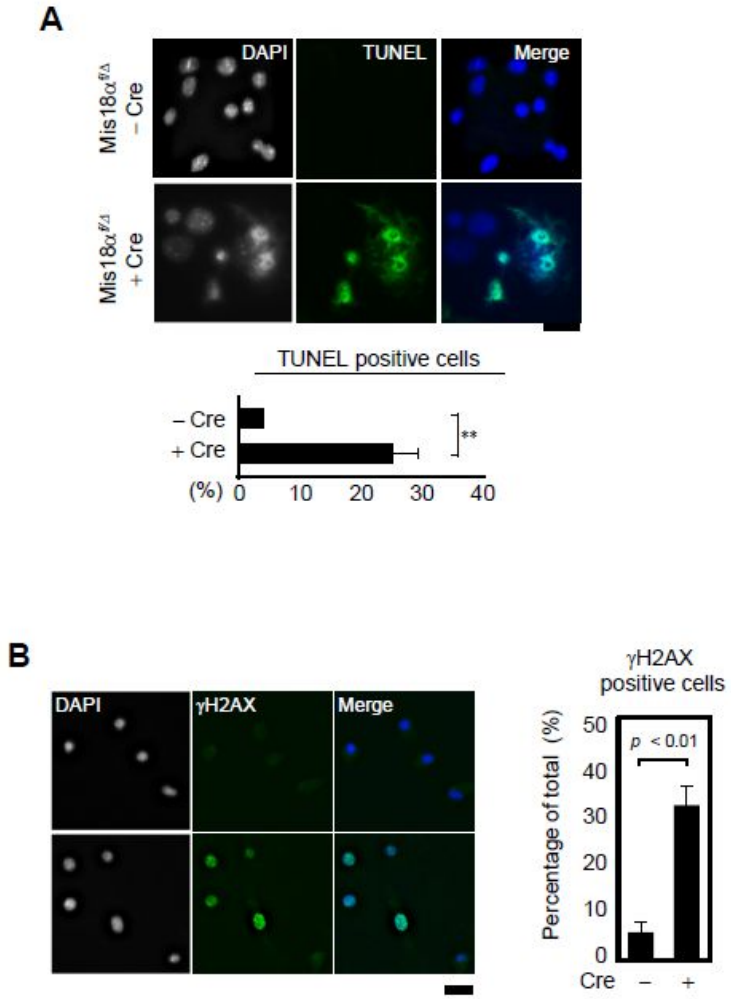

Figure II-10. Apoptosis and DNA damage was found in Mis18α-deficient MEFs
(A) TUNEL assay in *Mis18α*$^{f/\Delta}$ (–Cre) and *Mis18α*$^{\Delta/\Delta}$ (+Cre) MEFs. TUNEL positive cells were stained green and DAPI (blue) was for nuclei. Bottom histogram shows percentage of TUNEL positive cells, which is generated from counting 200 cells. P-value is calculated by t-test (∗ : $p < 0.05$). Scale bar: 40 μm. (B) γH2AX was stained to analyze DNA damage in Mis18α-deficient MEFs. γH2AX positive cells were stained green and DAPI (blue) was for nuclei. Right side histogram shows percentage of γH2AX positive cells, which is generated from counting 200 cells. P-value is calculated by t-test (∗ : $p < 0.05$). Scale bar: 20 μm.

Centromeric Localization of CENP-A, HJURP and Mis18α in Mouse Cells

In human cells, Mis18α localized with CENP-A during late mitosis or early G1 stages (Fujita et al., 2007). To confirm that the centromere localization of Mis18α was also recapitulated in my systems, immunocytochemistry was performed in different cell cycle stages. As it was reported, the dot-like staining pattern of Mis18α was found only in late mitosis or early G1 stages (Fig. II-11A). Colocalization between CENP-A and Mis18α in late mitosis was also confirmed (Fig. II-11B). To verify whether colocalization between CENP-A and Mis18α is occurred in centromere region, anti-centromere antibody (ACA) was used for centromere recognition (Fig. II-11C). ACA was a purified antibody from patient suffering autoimmune disease and it was confirmed that ACA specifically recognized centromere. As a results, Mis18α was also colocalized with ACA as well as with CENP-A. These staining results suggested that Mis18α specifically localized in centromere during late mitosis and it was well conserved in this system. Although mitosis-specific localization of CENP-A, HJURP and Mis18α is well known in human cells, there was no information about whether this localization was conserved in mouse cells. Since the timing of CENP-A loading varies depending on cell types and developmental stages (Carroll et al., 2010; Fukagawa et al., 2001; Kwon et al., 2007; Nishihashi et al., 2002), the cell cycle dependent distribution of Mis18α, HJURP and CENP-A was checked in MEFs. As in human cells, Mis18α, centromeric localization of HJURP and newly synthesized CENP-A was observed from late mitosis to early G1 in MEFs (Fig. II-12A, II-12B, and

II-12C). The centromeric localization of Mis18α and HJURP at late mitosis/early G1 was further confirmed by ChIP assay using synchronized cells (Fig. II-12D and II-12E). Therefore, as suggested for NIH3T3 cells whose LacI-HJURP was able to recruit CENP-A to the LacO array (Barnhart et al., 2011), localization dynamics of Mis18α and HJURP and the timing of CENP-A loading are well conserved in mouse cells as in human cells.

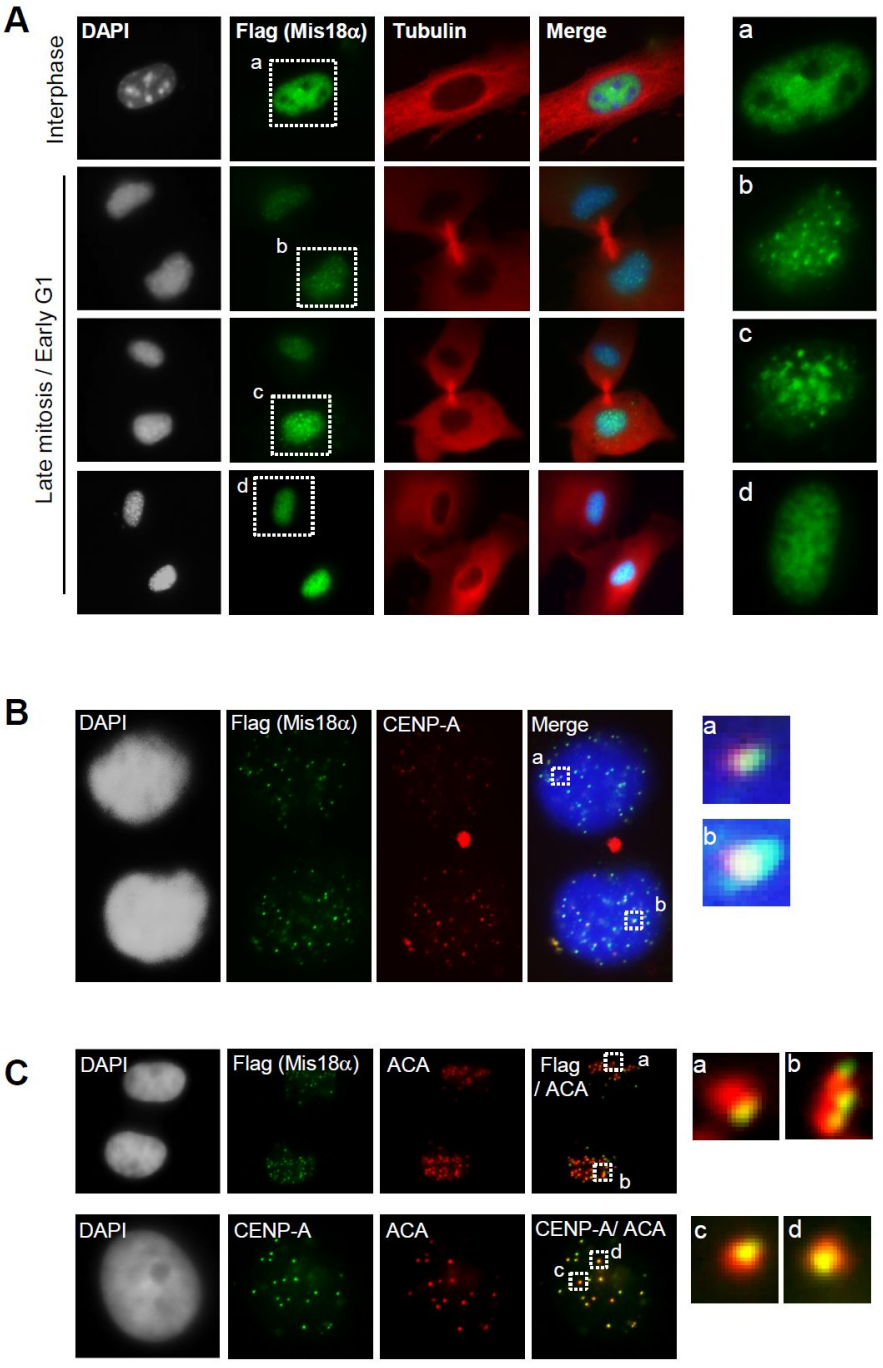
A
Interphase
Late mitosis / Early G1
DAPI
Flag (Mis18α)
Tubulin
Merge
a
b
c
d
B
DAPI
Flag (Mis18α)
CENP-A
Merge
a
b
C
DAPI
Flag (Mis18α)
ACA
Flag / ACA
CENP-A
CENP-A/ ACA

Figure II-11. Centromeric Localization of Mis18α

(A) Immunocytochemistry of Mis18α at different cell cycle stages after transfection of Flag-Mis18α in HeLa cells. Antibodies against α-Flag (green) and α-Tubulin (red) were used. Nuclei were stained with DAPI (blue). The insets were magnified to right side. (B) Immunocytochemistry was performed as in (A) except antibodies against α-Flag (green) and α-CENP-A (red) were used. Nuclei were stained with DAPI (blue). The insets in merged images were magnified to right side. (C) Centromeric localization of Mis18α was confirmed by ACA (anti-centromere antibody) staining. Immunocytochemistry was performed for colocalization between Mis18α (Green) and ACA (red) (upper panel). CENP-A (Green) was colocalized with ACA (red). The insets were magnified to right side.

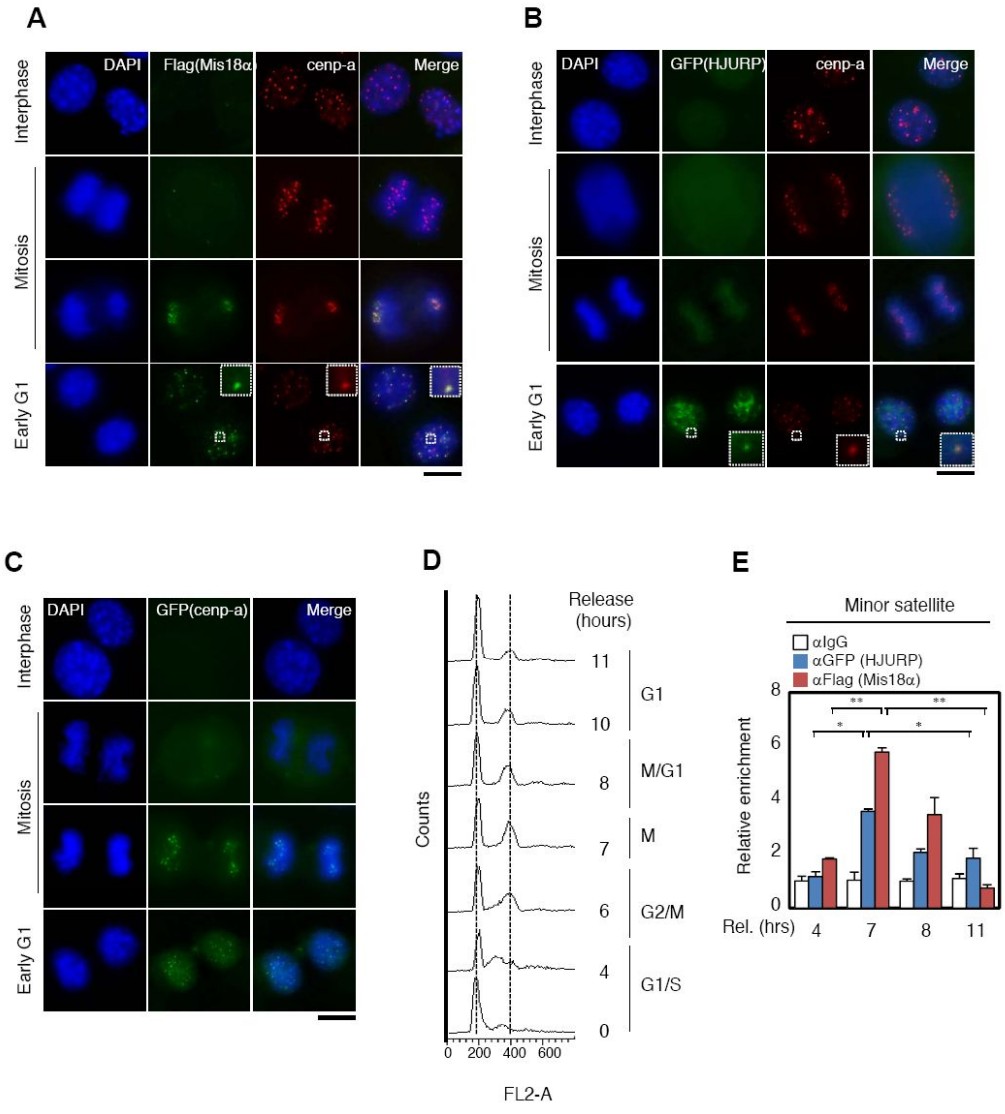
A
DAPI
Flag(Mis18α
cenp-a
Merge
Interphase
Mitosis
Early G1
B
DAPI
GFP(HJURP)
cenp-a
Merge
Interphase
Mitosis
Early G1
C
DAPI
GFP(cenp-a)
Merge
Interphase
Mitosis
Early G1
D
Release (hours)
11
10
8
7
6
4
0
G1
M/G1
M
G2/M
G1/S
Counts
0 200 400 600
FL2-A
E
Minor satellite
αIgG
αGFP (HJURP)
αFlag (Mis18α)
Relative enrichment
Rel. (hrs) 4 7 8 11

Figure II-12. The Timing for CENP-A Loading and Involvement of HJURP and Mis18α in Mouse Cells

(A) Immunocytochemistry of Mis18α and CENP-A at different cell cycle stages after transfection of Flag-Mis18α in NIH3T3 cells. Antibodies against α-Flag (green) and α-CENP-A (red) were used to visualize Mis18α and centromere, respectively. Nuclei were stained with DAPI (blue). The insets represent co-localized images indicated by dotted box. Scale bar: 10 μm. (B) Immunocytochemistry was performed after transfection of GFP-HJURP as in (A). Scale bar: 10 μm. (C) The loading of newly synthesized CENP-A was monitored using immunocytochemistry in NIH3T3 cells transiently transfected with GFP-CENP-A for 12 or 24 hrs. (D) NIH3T3 cells were synchronized by double thymidine block and DNA contents were analysed by flow cytometry (FACS) to determined cell cycle stages. (E) NIH3T3 cells expressing both Flag-Mis18α and GFP-HJURP were prepared at indicated time points after being released from double thymidine block. Chromatin fractions were immunoprecipitated with anti-Flag, anti-GFP or nonspecific IgG. Bound DNAs were quantified by real-time PCR with specific primers against Minor satellite repeat regions. The values are expressed as mean ± SEM of three independent experiments and calculated by t-test. $* : p < 0.05$, $** : p < 0.01$.

Distribution Pattern of Centromeric Histone Modification was Altered in *Mis18α*$^{\Delta/\Delta}$ MEFs.

Mis18α is neither an interacting partner of CENP-A nor a component of CENP-A complex, indicating it is distinct from CENP-A deposition factors such as HJURP (Dunleavy et al., 2009; Foltz et al., 2006; Fujita et al., 2007). Based on relatively earlier deposition of Mis18α than CENP-A (Fujita et al., 2007; Silva and Jansen, 2009), one possible mode of Mis18α action could be achieved by the establishment of centromeric chromatin signature through dynamic regulation of the epigenetic status. To test this possibility, epigenetic signature of centromeric chromatin in *Mis18α*$^{f/\Delta}$ MEFs was compared with that of *Mis18α*$^{+/\Delta}$ MEFs after Cre-introduction. Immunocytochemistry was performed using MEFs arrested at mitosis so that the defects of centromere region could be visualized clearly when chromosomes were condensed. It has been reported that the tri-methylation of H3K9, a marker for pericentric heterochromatin, is also detected from centromeric heterochromatin (Guenatri et al., 2004). Interestingly, the tri-methylation of H3K9 was reduced and broadly dispersed without specific enriched localization along chromosomes at prometaphase in *Mis18α*$^{\Delta/\Delta}$ MEFs (Fig. II-13, right panel), in contrast to forming bright dots and being concentrated at the center of the condensed chromosomes in *Mis18α*$^{+/\Delta}$ MEFs (Fig. II-13, left panel). This observation led us to examine the changes of epigenetic status in centromeric chromatin caused by Mis18α deficiency.

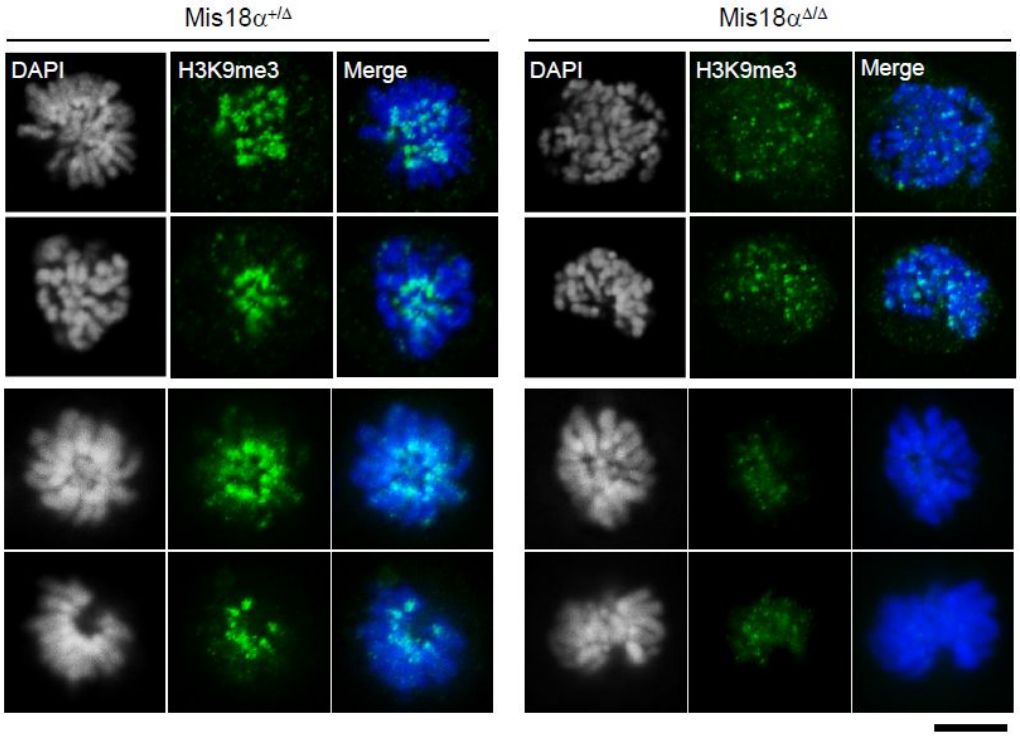

Figure II-13. Distribution of H3K9me3 during prometaphase in *Mis18α*$^{Δ/Δ}$ MEFs
Immunocytochemistry was performed to detect H3K9me3 (green) in Cre-expressing *Mis18α*$^{+/Δ}$ (*Mis18α*$^{+/Δ}$) or *Mis18α*$^{f/Δ}$ MEFs (*Mis18α*$^{Δ/Δ}$). DAPI (blue) was used to stain chromosomes. Prophase cells were collected after release from double thymidine block. Scale bar: 10 μm.

Mis18α is Crucial for Regulating Histone Modification and Noncoding Transcripts in Centromeric Chromatin

Because genomic structure or gene expression was governed by chromatin compaction through epigenetic status of histones, there are possibilities that modification of centromeric histone might be altered in *Mis18α*-deficient MEFs. To prove this possibility, chromatin immunoprecipitation (ChIP) assays were performed to analyze the methylation and acetylation status of centromeric histones using primer sets for minor satellite repeats (centromere region) in MEFs. Before analysis about epigenetic changes, it was validated whether the ChIP assay reproduces the loss of CENP-A in centromere region of *Mis18α*$^{\Delta/\Delta}$ MEFs. The localization of CENP-A in minor satellite repeats was significantly reduced in *Mis18α*$^{\Delta/\Delta}$ MEFs without any changes of total level of CENP-A, while H3 level was not changed in the same condition, confirming the importance of Mis18α in centromeric localization of CENP-A (Fig. II-14A). Given that excessive heterochromatin or euchromatin has been shown to disrupt centromere function (Nakano et al., 2008), epigenetic marker for silenced or open chromatin state of centromere was examined. The methylation levels of H3K9 (H3K9me2 and H3K9me3) were decreased in *Mis18α*$^{\Delta/\Delta}$ MEFs compared to *Mis18α*$^{f/\Delta}$ MEFs, whereas acetylation of H3 was increased (Fig. II-14B). Further, di-methylation of H3K4 (H3K4me2), which has been suggested to be required for HJURP targeting and CENP-A assembly (Bergmann et al., 2011), was also reduced in the centromere of *Mis18α*$^{\Delta/\Delta}$ MEFs.

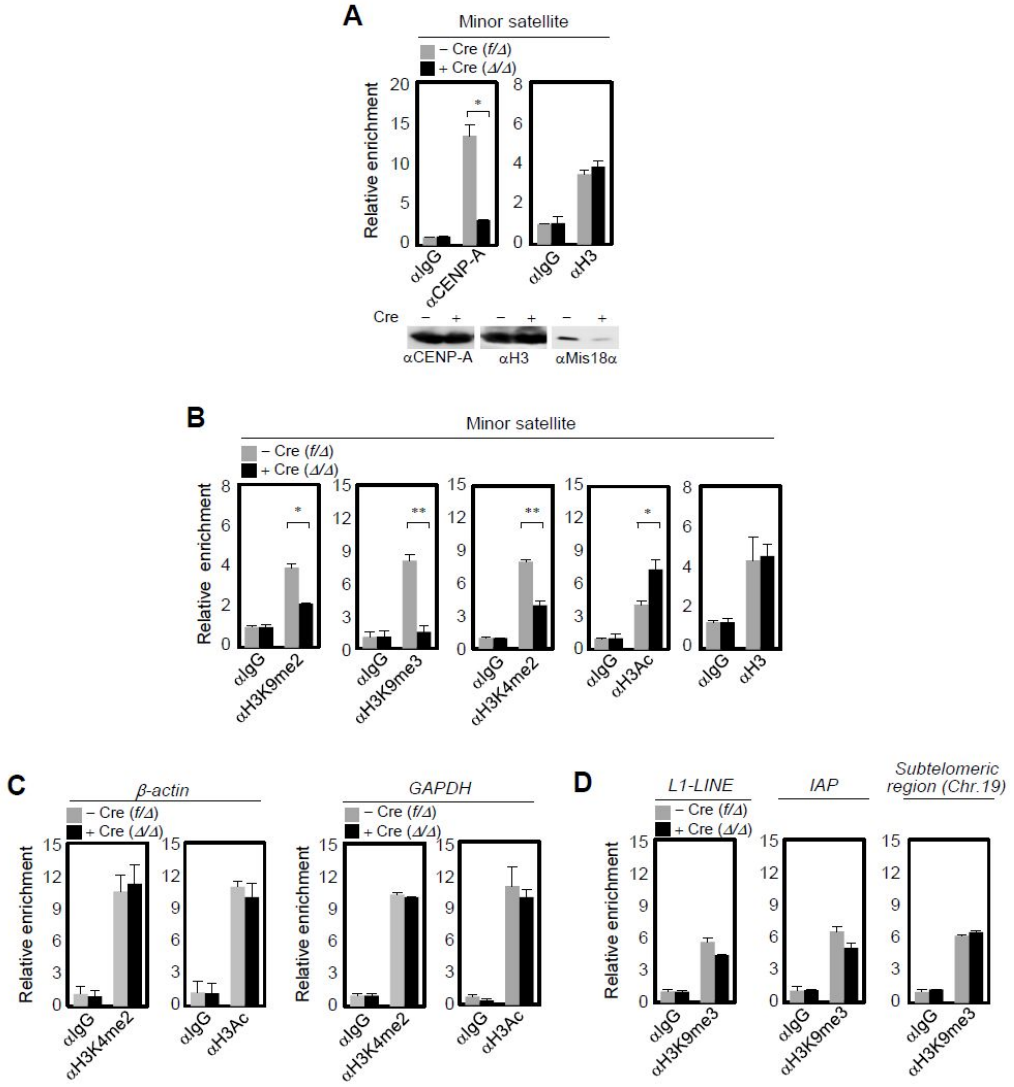
A
Minor satellite
– Cre (f/Δ)
+ Cre (Δ/Δ)
Relative enrichment
αIgG
αCENP-A
αIgG
αH3
Cre
αCENP-A
αH3
αMis18α
B
Minor satellite
αH3K9me2
αH3K9me3
αH3K4me2
αH3Ac
αH3
C
β-actin
GAPDH
αH3K4me2
αH3Ac
D
L1-LINE
IAP
Subtelomeric region (Chr.19)
αH3K9me3

Figure II-14. Histone modification patterns in centromere region of *Mis18α*-deficient MEFs

(A) ChIP assays were performed with chromatin fractions of *Mis18α*$^{f/\Delta}$ MEFs, which were generated before or after Cre-expression, using anti-CENP-A, anti-histone H3, or nonspecific IgG as a control. Bound DNAs were quantified by real-time PCR with specific primers against minor satellite repeat regions. Relative enrichment values were calculated by normalizing to relative DNA input and expressed as fold enrichment to IgG. The values are expressed as mean ± SEM of three independent experiments. ∗ : $p < 0.05$, ∗∗ : $p < 0.01$. The total levels of CENP-A, H3 and Mis18α in starting material of ChIP sample were shown in the bottom using immunoblot assay. (B) ChIP assays were performed as in (A) using antibodies against H3K9me2, H3K9me3, H3K4me2, H3Ac, histone H3, or nonspecific IgG. (C and D) Control ChIP assays were conducted as in (B) using indicated antibodies in various regions away from centromere, including β-actin and GAPDH in (C) and LINE-1, IAP, sub-telomeric region of chromosome 19 (Chr.19) in (D).

However, there was little or no difference between WT and Mis18α KO cells for the representative euchromatic regions including housekeeping gene promoter regions of *β-actin* and *GAPDH* (Fig. II-14C), and heterochromatic regions including DNA repeat sequence regions (LINE-1 and IAP) and sub-telomeric regions (Chr. 19) (Fig. II-14D). These data suggest that the altered chromatin state in Mis18α KO cells is specific for the centromeric region. Next, the levels of heterochromatin-associated proteins were analyzed in the same context. Centromeric recruitment of histone methyltransferases (HMTs) such as those responsible for tri-methylating H3K9 (SUV39H1) and mono- or di-methylating H3K9 (G9a/GLP) was reduced in *Mis18α*$^{\Delta/\Delta}$ MEFs (Fig. II-15A). H3K9me3 reader HP1α and HP1β were also reduced in *Mis18α*$^{\Delta/\Delta}$ MEFs. In addition, decreased recruitment of histone deacetylase HDAC1 supported increased level of H3 acetylation. Therefore, these results suggest that Mis18α is involved in the regulation of histone modification in centromeric chromatin for CENP-A loading.

It has been shown that the transcripts produced from satellite repeats in centromere region are increased in disrupted centromeric chromatin (Bouzinba-Segard et al., 2006; Zhang et al., 2008). As a measure of defective histone modifications in centromeric chromatin, noncoding transcript levels were analyzed in *Mis18α*$^{\Delta/\Delta}$ MEFs by quantitative RT-PCR. Depletion of Mis18α led to the increased centromeric noncoding transcripts (Fig. II-15B). However, there was no change in the transcripts level when deletion was made in *Mis18α*$^{f/\Delta}$ MEFs stably expressing ectopic

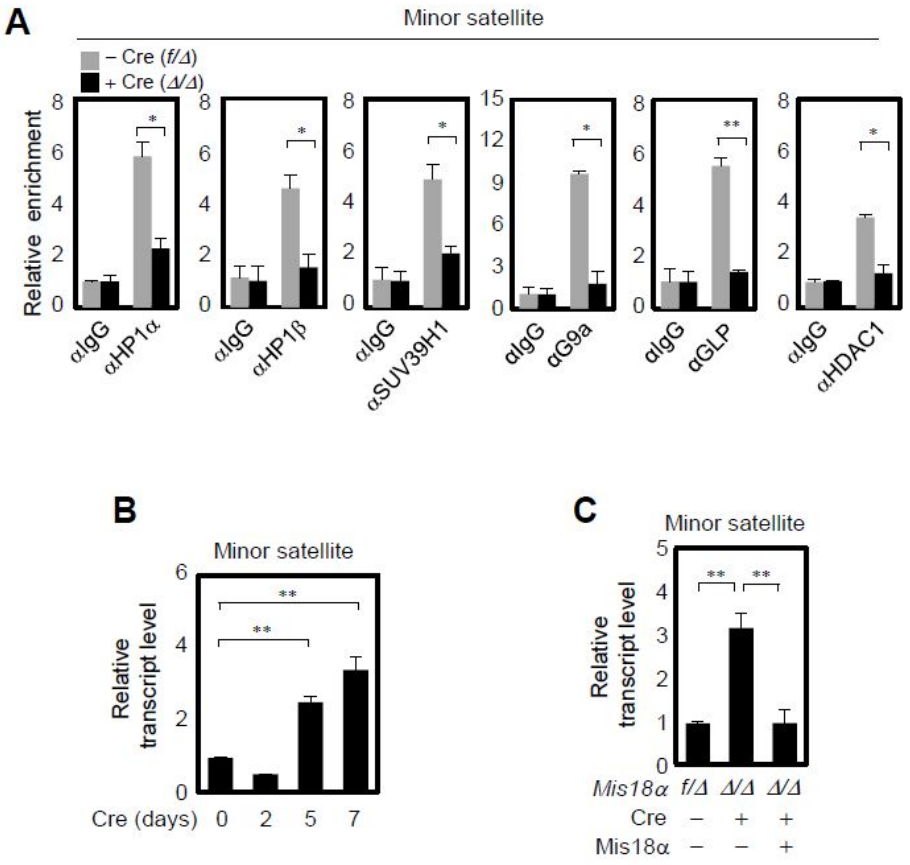

Figure II-15. Disrupted Centromeric Chromatin in centromere region of *Mis18α*-deficient MEFs

(A) ChIP assays were performed with chromatin fractions of *Mis18α*$^{f/\Delta}$ MEFs, which were generated before or after Cre-expression, using indicated antibodies. (B) Quantitative RT-PCR was performed to define transcript levels from centromere region of MEFs. (C) Quantitative RT-PCR analysis was performed as in (B) using *Mis18α*$^{f/\Delta}$ MEFs reconstituted with Mis18α after Cre-expression.

Mis18α (Fig. II-15C), suggesting that the increased levels of centromeric transcripts in *Mis18α*-deficient MEFs is mainly due to the lack of Mis18α. Therefore, Mis18α plays an important role in maintaining centromeric chromatin states and regulating noncoding transcripts during cell division. Given that the loss of CENP-A at centromere in Mis18α knockdown cells is recovered by TSA, a HDAC inhibitor (Fujita et al., 2007), the TSA effect on Mis18α KO MEFs was examined. Unlike knockdown system, CENP-A loading problem failed to be rescued by TSA treatment in Mis18α KO MEFs (Fig. II-16A and II-16B). Thus, it was speculated that TSA treatment might not be sufficient to rescue the loss of CENP-A localization in Mis18α KO systems compared to the TSA effect shown in knockdown system.

Mis18α Interacts with DNMT3A/3B through its C-terminal Leucine Rich Region

Since altered epigenetic marks were observed in the centromere of *Mis18α*-deficient MEFs, I set out to find Mis18α interacting proteins which are related to histone modifications. None of histone methyltransferases (HMTs), histone demethylases (HDMs), or HP1 proteins interacted with Mis18α (Fig. II-17A). Mis18α was able to interact with DNMTs, namely DNMT3A and DNMT3B but not DNMT1. These interactions were confirmed at endogenous expression levels (Fig. II-17B). DNaseI treatment did not affect the binding of Mis18α to DNMT3A/3B (Fig. II-17C), indicating that their interaction is not mediated by the presence of DNA.

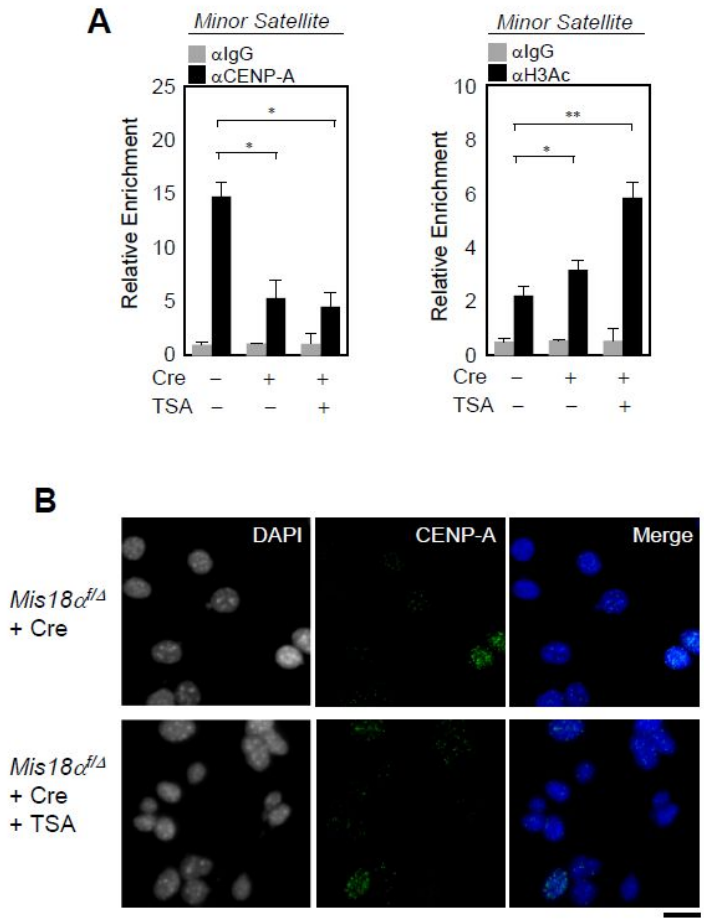

Figure II-16. CENP-A Mislocalization in *Mis18α*$^{Δ/Δ}$ MEFs Is Not Suppressed by TSA

(**A**) ChIP assays were performed with chromatin fractions of *Mis18α*$^{f/Δ}$ MEFs, which were generated before or after Cre-expression, using anti-CENP-A, anti-acetylated histone H3, or nonspecific IgG. Bound DNAs were quantified by real-time PCR with specific primers against minor satellite repeat regions. The values are expressed as mean ± SEM of three independent experiments. ∗ : $p < 0.05$, ∗∗ : $p < 0.01$. (**B**) Immunocytochemistry images of *Mis18α*$^{f/Δ}$ MEFs after Cre infection with or without treatment of TSA (50ng/ml). Antibodies against α-CENP-A (green) were used. DAPI (blue) was used to stain nucleus. Scale bar: 20 μm.

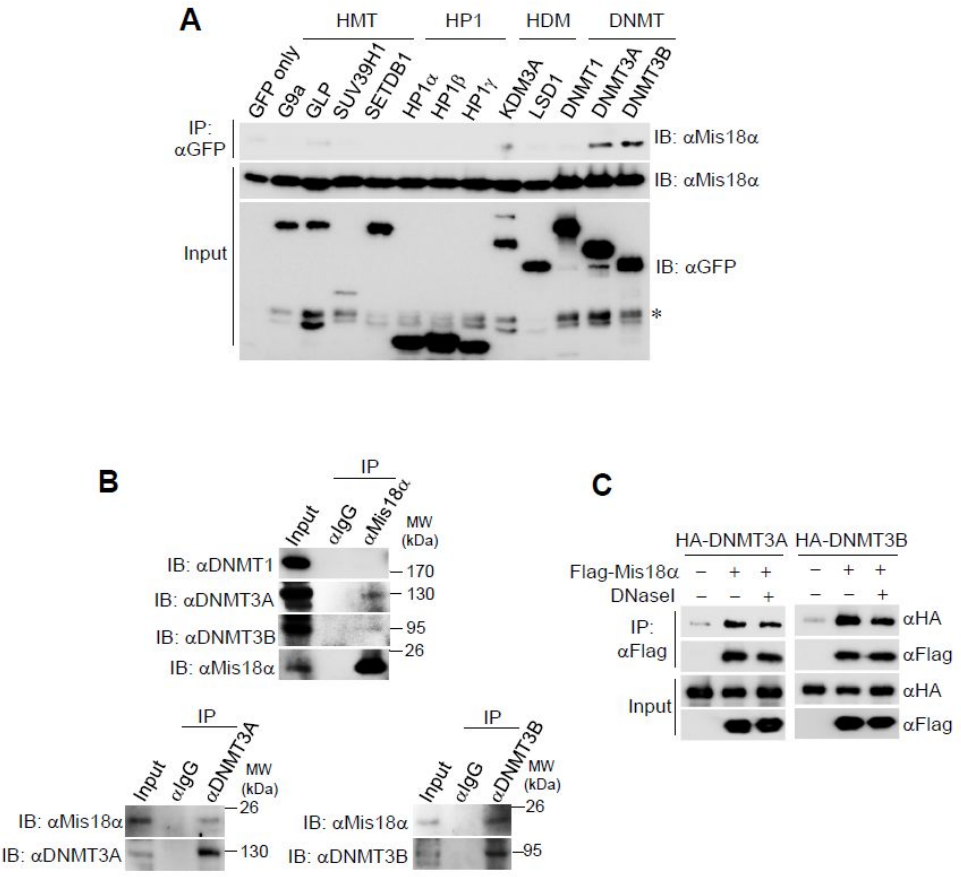

Figure II-17. Interaction between Mis18α and DNMT3A/3B without DNA

(A) Screening for Mis18α binding partners including various HMTs, HP1, HDMs, and DNMTs. Interactions were tested by coimmuniprecipitation in HEK293 cells transfected with Mis18α and candidate proteins in combination as indicated. The lower cross reacting band was marked by asterisk. (B) Coimmunoprecipitation assay was performed to detect endogenous interaction between Mis18α and DNMT3A/3B in NIH3T3 cells. (C) Coimmunoprecipitation assay between Mis18α and DNMT3A/3B was repeated with treatment of DNaseI (20 unit/ml) for 10 min at room temperature.

Next, it was analyzed that which part of Mis18α is crucial for binding to DNMT3A/3B. For immunoprecipitation assay, three deletion mutants of Mis18α; DL1 (deletion of N-terminal region), DL2 (deletion of N-terminal region and cystein rich region which is known to influence CENP-A loading), and DL3 (deletion of C-terminal region) were generated. Among these deletion mutants, DL3 almost completely failed to bind DNMT3A/3B, indicating that the C-terminal region of Mis18α is crucial for its interaction with DNMT3A/3B (Fig. II-18A). Then, I searched for any putative protein-protein interaction motif in Mis18α and found leucine rich region (LRR)-like sequence, a framework for protein-protein interaction (Kobe and Kajava, 2001), at the end of the C-terminal region. In LRR-like region of Mis18α, 5 leucine residues are conserved in various organisms (Fig. II-18B). Interestingly, either deletion of LRR (ΔLRR) or replacement of 5 leucine residues at LRR by alanine (5LA) abrogated interaction between Mis18α and DNMT3A/3B (Fig. II-18C). Thus, the C-terminal LRR in Mis18α is critical for its binding to DNMT3A/3B.

Following questions were whether the 5LA mutant form of Mis18α (Mis18α5LA) which does not interact with DNMT3A/3B can replace endogenous Mis18α for the centromeric localization of CENP-A. Before analysis, the centromeric localization of wild-type (WT) or Mis18α5LA was validated. Both Mis18αWT and Mis18α5LA were localized in centromere region during early G1 phase in HeLa cells, suggesting that Mis18α5LA has a comparable potential for

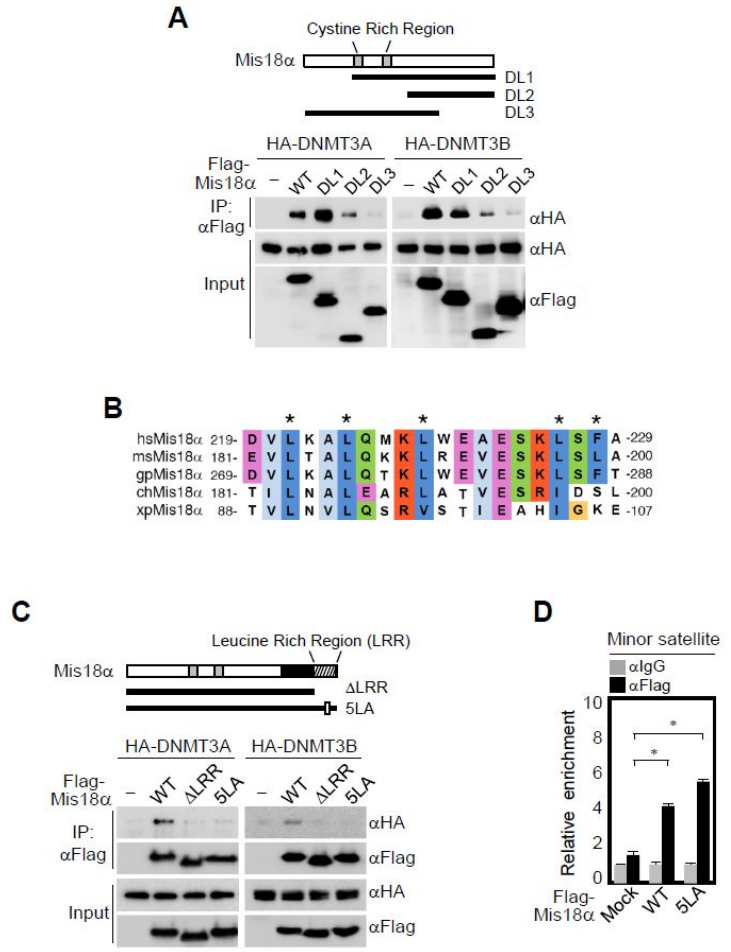

Figure II-18. Interaction between C-terminal LRR region of Mis18α and DNMT3A/3B

(A) Interactions between each deletion construct of Mis18α and either DNMT3A or DNMT3B were analyzed. (E) The leucine rich region in the C-terminus of Mis18α orthologs is aligned using ClustalW program. Conserved amino acids were highlighted with asterisk. (F) Interactions between DNMT3A/3B and WT, ΔLRR or 5LA mutant of Mis18α were analyzed. (G) ChIP assays were performed in HeLa cells stably expressing WT or 5LA mutant of Mis18α. Centromere occupancy by WT and 5LA mutant was analyzed. The values are expressed as mean ± SEM of three independent experiments. ∗ : $p < 0.05$.

centromeric localization compared to WT (Fig. II-18D).

To rule out the possibility that the integrity of the Mis18 complex may be affected by 5LA mutation, the interaction between them was verified. Both Mis18αWT and Mis18α5LA exhibited the comparable binding to Mis18BP1, Mis18β, and DNMT3A/3B (Fig. II-19A, II-19B and II-19C). Further, the fusion proteins of Mis18β/Mis18α were generated to eliminate the possibility that slightly reduced binding between Mis18β and Mis18α5LA affects the loss of binding of Mis18α to DNMT3A/3B. Coimmunoprecipication assay revealed that the fusion protein of Mis18β/Mis18α5LA exhibited loss of binding to DNMT3A/3B (Fig. II-19D), suggesting that Mis18α5LA has a defect in DNMT3A/3B binding without affecting the integrity of the Mis18 complex. Then, the defects of CENP-A loading in *Mis18α*-deficient MEFs reconstituted with either WT or 5LA mutant were examined by immunocytochemistry. As expected, the loss of CENP-A dots by Mis18α deletion was rescued in MEFs stably expressing Mis18αWT (Fig. II-20). However, Mis18α5LA could not replace endogenous Mis18α for centromeric localization of CENP-A. These data suggest that the C-terminal LRR of Mis18α, which is critical for the interaction with DNMT3A/3B, is also indispensable for the centromeric localization of CENP-A. Thus, the interaction between Mis18α and DNMT3A/3B might play an important role in proper localization of CENP-A. However, it cannot be eliminated the possibility that failure to rescue using Mis18α 5LA mutant is, at least in part, due to slightly reduced Mis18α-Mis18β interaction as shown by Figure II-18B.

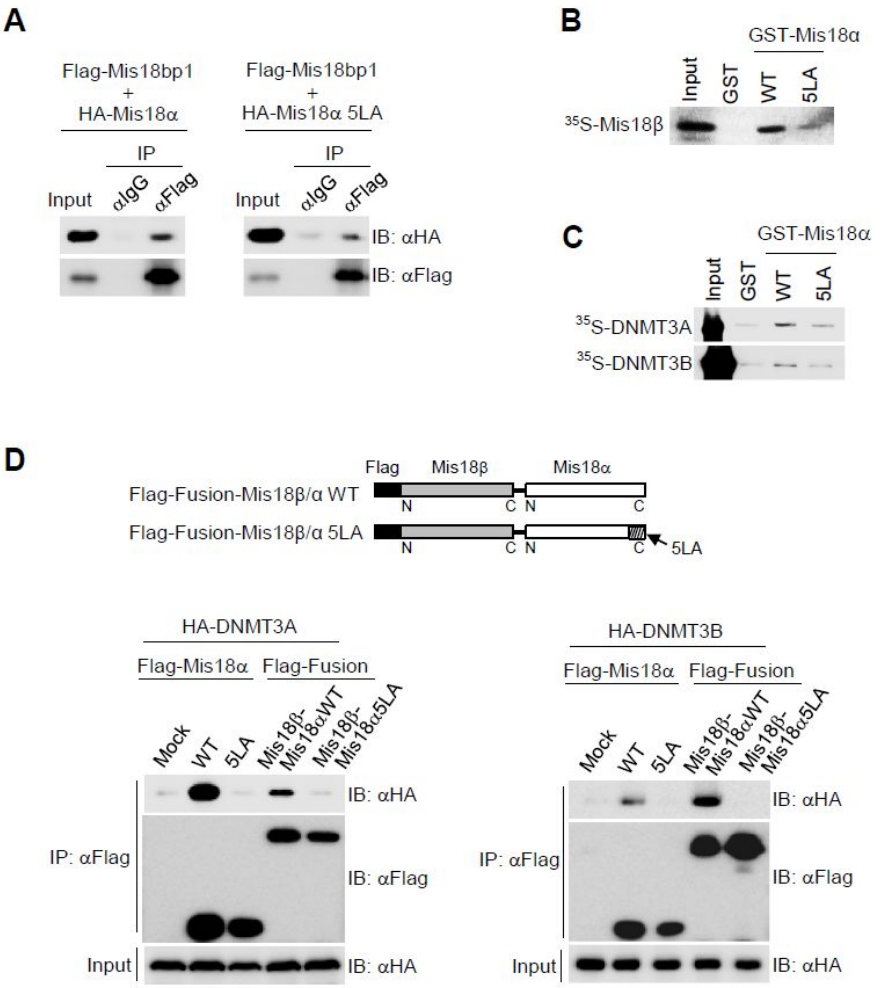

Figure II-19. The Integrity of Mis18 Complex Is Not Affected by Mis18α 5LA Mutant

(A) The binding affinity between Mis18α WT and 5LA mutant to Mis18BP1 was determined by coimmunoprecipitation assay in HEK293 cells transiently transfected with Mis18α, 5LA mutant and Mis18BP1. (B) The binding affinity between Mis18α and 5LA mutant to Mis18β was compared by GST pull-down assay. (C) GST pull assay was performed to detect direct binding between Mis18α and DNMT3A/3B. (D) Interactions of Mis18α-Mis18β fusion constructs to either DNMT3A or DNMT3B were analyzed by coimmuniprecipitation assays in HEK293 cells.

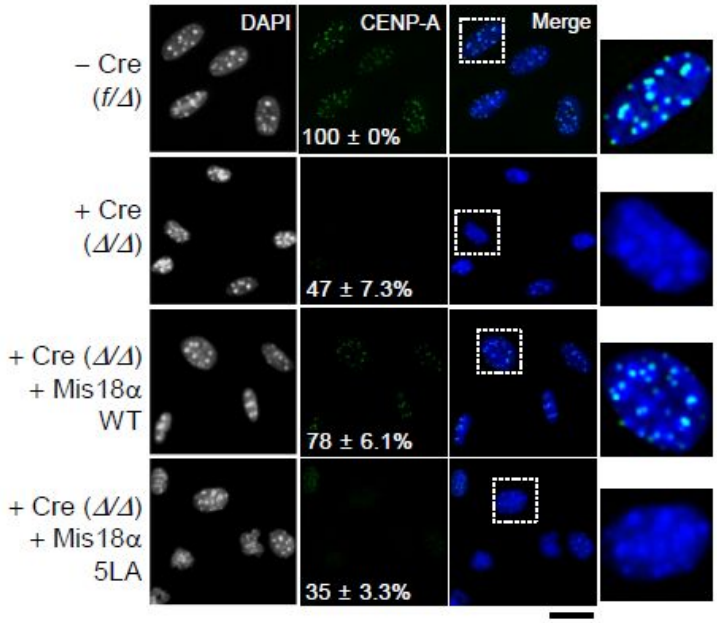

Figure II-20. LRR Region of Mis18α is Significant for CENP-A Loading to Centromere.

Immunocytochemistry images of *Mis18α*$^{f/\Delta}$ MEFs, stably expressing either WT or 5LA of Mis18α with or without Cre-expression. The percentage of cells showing CENP-A dots (green) was calculated by counting 400 cells. DAPI (blue) was used to stain nucleus. The insets are magnified to the right side. Scale bar: 20 μm.

Interaction between Mis18α and DNMT3A/3B Reinforces their Centromeric Localization

Based on the interaction between Mis18α and DNMT3A/3B, it was hypothesized that Mis18α and DNMT3A/3B are functionally linked for the regulation of the epigenetic status of centromeric chromatin. First, it was tested whether I can detect the temporal manner of Mis18α's centromeric localization using ChIP assay and then questioned whether centromeric DNMT3A/3B levels are variable during cell cycle. To answer the question, synchronized cells were harvested at indicated times after release from double thymidine block, and applied for ChIP analysis. In these assay, Mis18α was detected in the centromeric region with the peak at around 11 hr, which corresponds to early G1 stage of cell cycle, as expected (Fig. II-21A). Interestingly, the levels of centromeric DNMT3A/3B were increased from 9 to 11 hours after release (Fig. II-21B). Since the time frame of centromeric localization of Mis18α and DNMT3A/3B is overlapping, the interaction between Mis18α and DNMT3A/3B was examined during cell cycle. The interaction was most pronounced at 10 to 11 hours after cell cycle release (Fig. II-21C), which corresponds to the time frame for centromeric localization of Mis18α and DNMT3A/3B. To verify temporal dynamic interaction between Mis18α and DNMT3A/3B in centromeric region, a two-step ChIP assay was employed using the 10 or 11 hour sample from Figure III-10C. The result revealed that Mis18α and DNMT3A/3B exhibited mutual binding in centromeric region (Fig. II-21D).

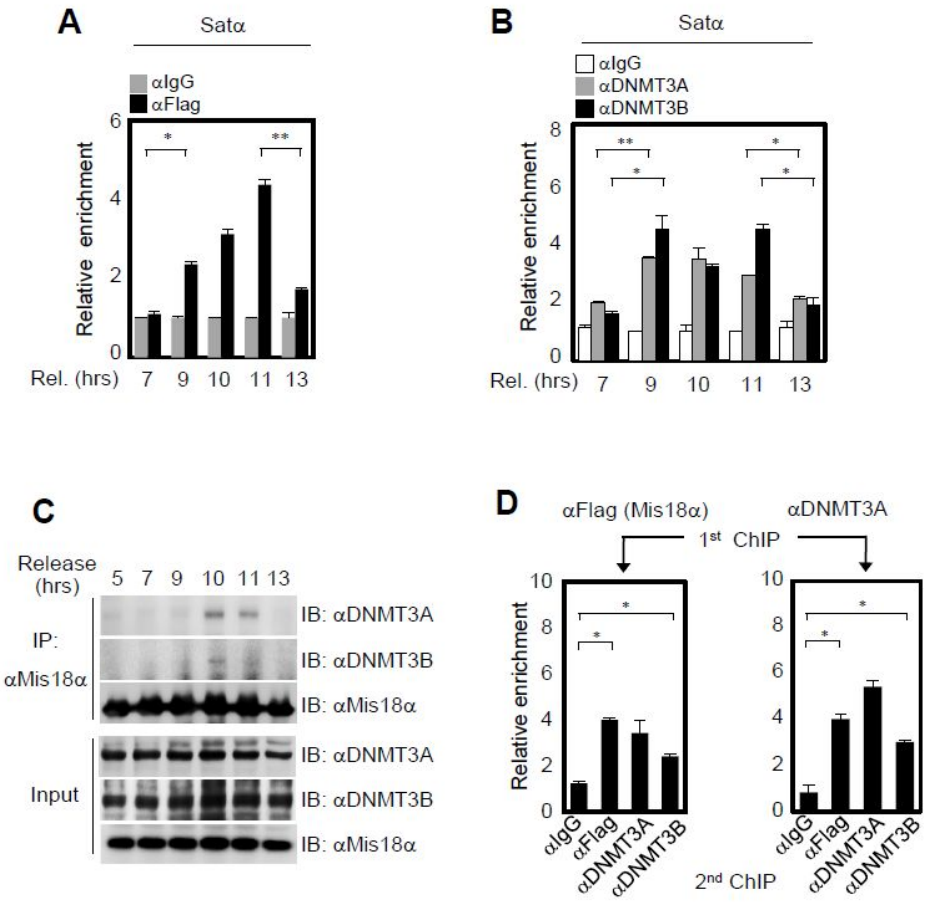

Figure II-21. The Mutual Binding and Centromeric Enrichment between Mis18α and DNMT3A/3B

(A and B) ChIP assays were performed in HeLa cells stably expressing Flag-Mis18α, which were prepared at indicated time points after being released from double thymidine block. Centromere occupancy by Mis18α (A), DNMT3A and DNMT3B (B) was analyzed. The values are expressed as mean ± SEM of three independent experiments. ∗ : $p < 0.05$, ∗∗ : $p < 0.01$. (C) The interactions between Mis18α and DNMT3A or DNMT3B were monitored by coimmunoprecipitation assays in HeLa cells, which was prepared as in (A). (D) Two-step ChIP assays were performed in HeLa cells stably expressing Mis18α. The chromatin fractions were first subject to pull-down with indicated antibodies, eluted from immuno-complexes, and applied for the second pull-down with the reciprocal antibodies.

To analyze whether the centromeric recruitment of DNMT3A/3B is altered by Mis18α, the centromeric localization of DNMT3A/3B was examined using ChIP assay after deletion of *Mis18α* from *Mis18α*$^{f/\Delta}$ MEFs. Indeed, DNMT3A/3B levels in centromere region were significantly reduced in *Mis18α*-deficient MEFs (Fig. II-22A), whereas the total amount of DNMT3A or DNMT3B protein was not altered (Fig. II-22B). Interestingly, knockdown of DNMT3A/3B caused decreased level of centromeric Mis18α (Fig. II-22C). Together, these results suggest that Mis18α and DNMT3A/3B cooperate for their centromeric localization.

The ability of Mis18αWT to localize DNMT3A/3B was compared with 5LA mutant of Mis18α in centromere region. Ectopic expression of WT resulted in elevated levels of DNMT3A/3B in centromere region as assessed by ChIP assay, whereas 5LA mutant did not enhance the centromeric localization of either DNMT3A or DNMT3B (Fig. II-22D). Further, the significance of the mutual interaction of these proteins was confirmed by the rescue experiment. Since it was found that the loss of Mis18α caused decreased centromeric localization of DNMT3A/3B, I asked whether WT or 5LA mutant could compensate for this decrease. ChIP analysis revealed that reduced levels of centromeric DNMT3A/3B in Mis18α-deprived condition were compensated by WT reconstitution, but not by Mis18α5LA (Fig. II-22E). Taken together, Mis18α and DNMT3A/3B colocalize at the centromere in mitosis to early G1 stage of cell cycle and cooperate to reinforce mutual localization in the region.

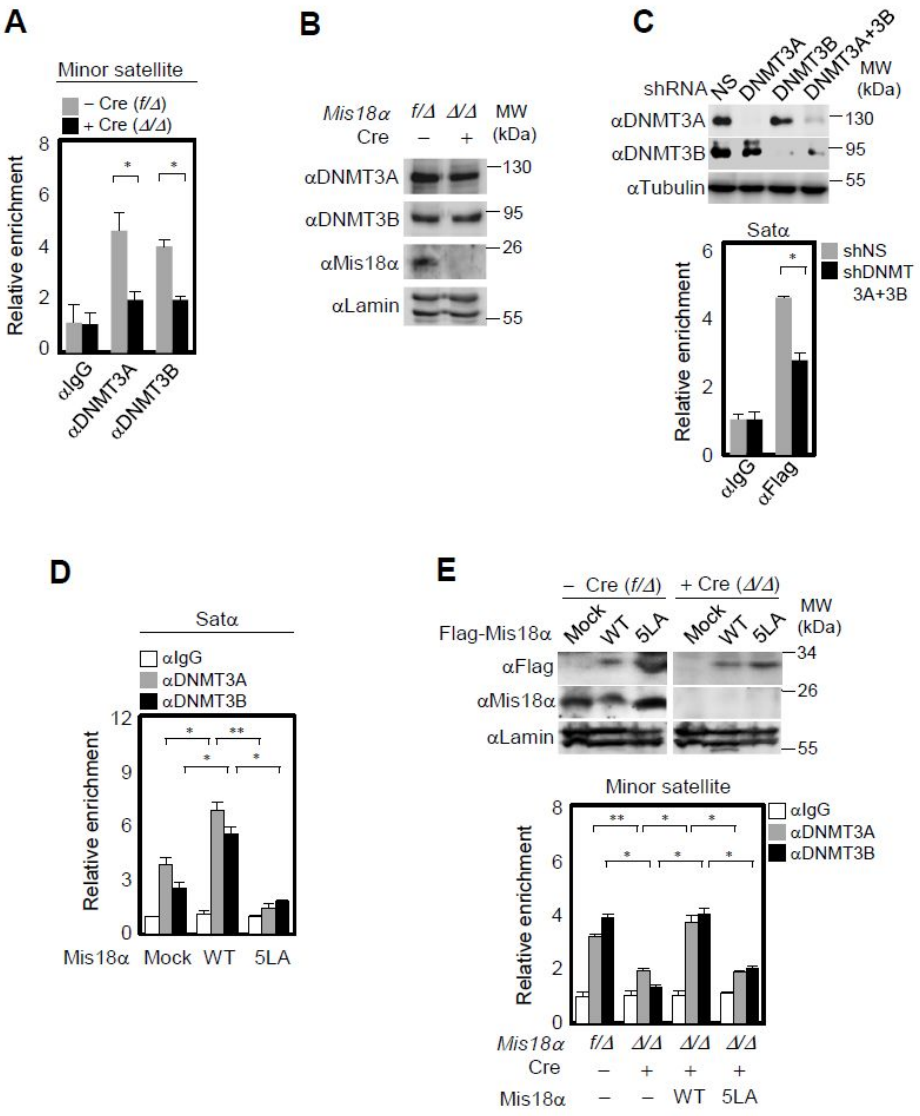
A
Minor satellite
– Cre (f/Δ)
+ Cre (Δ/Δ)
Relative enrichment
αIgG
αDNMT3A
αDNMT3B
B
Mis18α f/Δ Δ/Δ
Cre – +
MW (kDa)
αDNMT3A
αDNMT3B
αMis18α
αLamin
130
95
26
55
C
shRNA NS DNMT3A DNMT3B DNMT3A+3B
MW (kDa)
αDNMT3A
αDNMT3B
αTubulin
130
95
55
Satα
shNS
shDNMT 3A+3B
Relative enrichment
αIgG
αFlag
D
Satα
αIgG
αDNMT3A
αDNMT3B
Relative enrichment
Mis18α Mock WT 5LA
E
– Cre (f/Δ)
+ Cre (Δ/Δ)
Flag-Mis18α Mock WT 5LA Mock WT 5LA
MW (kDa)
αFlag
αMis18α
αLamin
34
26
55
Minor satellite
αIgG
αDNMT3A
αDNMT3B
Relative enrichment
Mis18α f/Δ Δ/Δ Δ/Δ Δ/Δ
Cre – + + +
Mis18α – – WT 5LA

Figure II-22. Centromeric localization of DNMT3A/3B and Mis18α is facilitated by their interaction

(A) ChIP assays were performed in *Mis18α*$^{f/\Delta}$ MEFs before or after Cre-expression. Centromere occupancy by DNMT3A and DNMT3B was analyzed. The values in (A) and (B)-(E) are expressed as mean ± SEM of three independent experiments. ∗ : $p < 0.05$, ∗∗ : $p < 0.01$. (B) Immunoblot analysis to compare protein levels of DNMT3A and DNMT3B in *Mis18α*$^{f/\Delta}$ MEFs with or without Cre-expression. (C) ChIP assays were performed in HeLa cells stably expressing Flag-Mis18α with mixed shRNAs against DNMT3A and DNMT3B. Centromere occupancy by Mis18α was analyzed. (D) ChIP assays were performed in HeLa cells transfected with vector only, WT, or 5LA mutant of Mis18α. Centromere occupancy by DNMT3A and DNMT3B was analyzed. (E) ChIP assays were performed in *Mis18α*$^{f/\Delta}$ MEFs stably expressing WT or 5LA in with or without of Cre-expression. Centromere occupancy by DNMT3A and DNMT3B was analyzed.

CENP-C Is Not Directly Required for the Licensing Function of Mis18α in Association with DNMT3A/3B at Centromeres

Since the constitutive centromere protein CENP-C has been shown to recruit DNMT3B to centromeres (Gopalakrishnan et al., 2009) and affect centromeric localization of Mis18BP1 (Moree et al., 2011), it was explored whether CENP-C is required for the Mis18α function in association with DNMT3A/3B. To verify the interaction between CENP-C and Mis18 complex, co-immunoprecipitation assay was performed and confirmed that CENP-C bound to Mis18 complex including Mis18BP1 and Mis18α (Fig. II-23A). Further, both Mis18αWT and Mis18α5LA exhibited comparable binding to CENP-C (Fig. II-23B), suggesting that Mis18α5LA has a defect in DNMT3A/3B binding while preserving its interaction with CENP-C. To examine whether the Mis18α and DNMT3A/3B interaction is through CENP-C, coimmunoprecipitation assay was performed using CENP-C-depleted cell extracts. The binding of Mis18α to DNMT3A/3B was not affected by knockdown of CENP-C (Fig. II-23C). Then, it was examined whether Mis18α affects the CENP-C and DNMT3A/3B interaction. There was little or no difference of the binding between CENP-C and DNMT3A/3B in WT and Mis18α KO cells (Fig. II-23D). Further, overexpression of Mis18α did not affect the binding between CENP-C and DNMT3A/3B (Fig. II-23E).

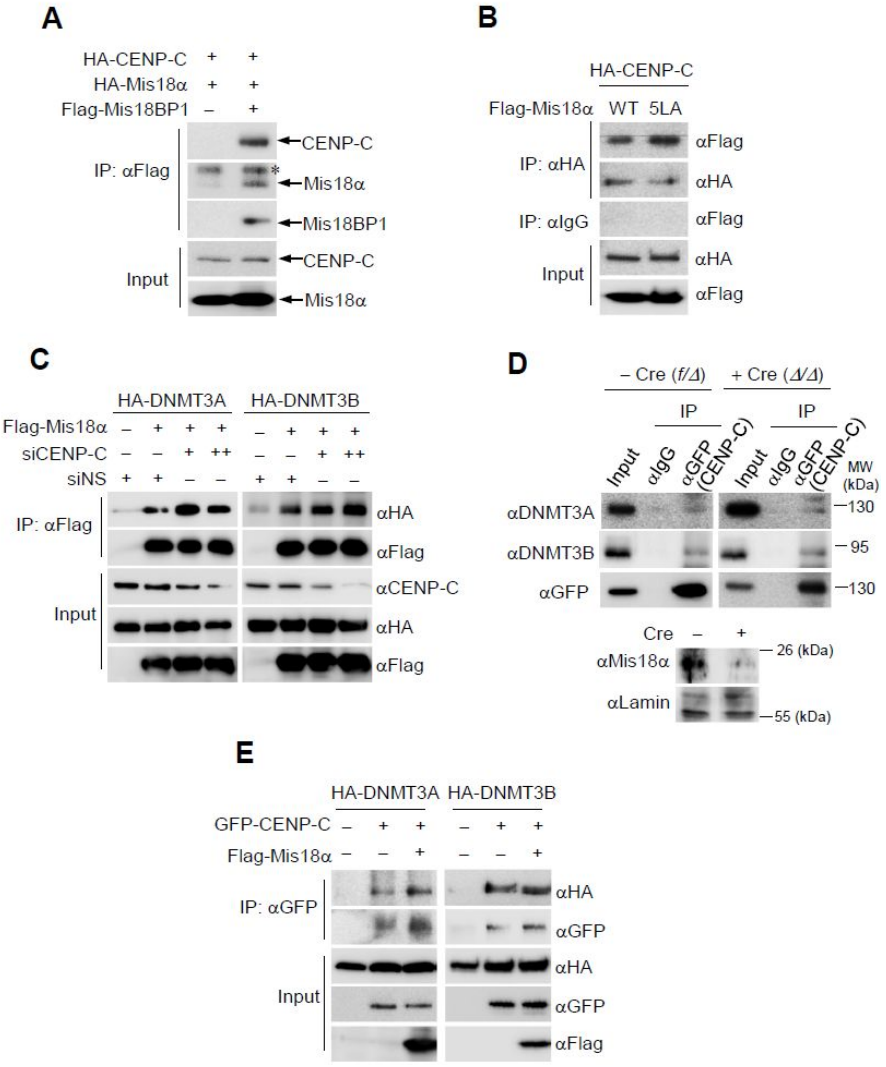

Figure II-23. DNMT3A/3B/Mis18 Complex is independent of CENP-C /DNMT3A/3B complex.

(A) Coimmunoprecipitation of Mis18 complex with CENP-C. (B) Coimmunoprecipitation of Mis18α WT or 5LA mutant with CENP-C. (C) The interaction between Mis18α and DNMT3A/3B was not affected by knock-down of CENP-C. (D) CENP-C-DNMT3A/3B interaction in *Mis18α*$^{f/\Delta}$ and *Mis18α*$^{\Delta/\Delta}$ MEFs. (E) The interaction between CENP-C and DNMT3A/3B was not affected by ectopic expression of Mis18α in HEK293 cells.

Next, I explored whether Mis18α stabilizes or enhances CENP-C. *Mis18α*-deficiency did not alter the protein stability of CENP-C (Fig. II-24A). ChIP assay conducted on the minor satellite region revealed that CENP-C enrichment was significantly decreased without Mis18α (Fig. II-24B). To determine whether the reduced CENP-C enrichment in Mis18α KO cells is due to the loss of CENP-A localization rather than Mis18α localization, ChIP assay was performed to monitor CENP-A and CENP-C enrichment in the minor satellite region after transfecting MEFs with CENP-A or CENP-C siRNA (Fig. II-24C). While CENP-C enrichment was significantly decreased in CENP-A knockdown MEFs, CENP-A enrichment was slightly changed by the loss of CENP-C as was previously reported (Carroll et al., 2010). Although CENP-C conducts an important role in centromeric localization of Mis18 complex, the interaction between Mis18α and DNMT3A/3B and CENP-A loading by them appear to be CENP-C- independent.

Decreased DNA Methylation by *Mis18α*-Deficiency Leads to the Impaired Centromeric Localization of CENP-A

It has been shown that *Dnmt3a/3b* deletion led to reduced DNA methylation of pericentric heterochromatin (Chen et al., 2004), and the loss of DNMT3B has been reported to cause increased transcription of centromeric repeats and chromosome segregation defect during mitosis (Gopalakrishnan et al., 2009). Therefore, the reduced centromeric localization of DNMT3A/3B in *Mis18α*-deficient MEFs raised

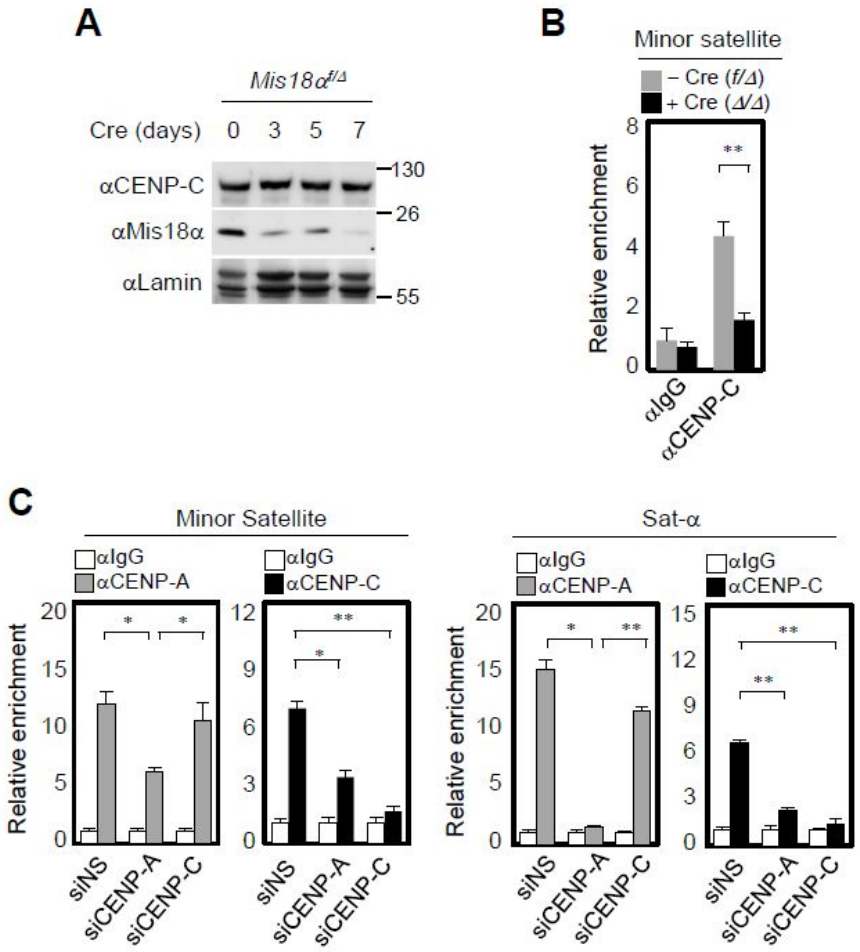

Figure II-24. CENP-C is not directly required for Mis18α-dependent localization of DNMT3A/3B at centromeres

(A) The stability of CENP-C proteins in the absence of Mis18α. (B) ChIP assays were performed in *Mis18α*$^{f/\Delta}$ MEFs with or without Cre infection. Centromere occupancy by CENP-C was analyzed. The values in (G) and (H) are expressed as mean ± SEM of three independent experiments. ∗ : $p < 0.05$, ∗∗ : $p < 0.01$. (C) ChIP assays were performed in *Mis18α*$^{f/\Delta}$ MEFs or HeLa cells transfected with indicating siRNAs. Centromere occupancy by CENP-A and CENP-C was analyzed.

the possibility that hypomethylation of centromeric DNAs in *Mis18α*-deficient cells might cause perturbation of heterochromatin architecture, leading to CENP-A loading problem. To test this possibility, the methylation status of the centromere region was analyzed in MEFs. In accordance with the decreased level of centromeric DNMT3A/3B in *Mis18α*$^{\Delta/\Delta}$ MEFs as shown in Figure III-11A, the overall PCR products after *Mae*II or *Hpa*II digestion were reduced in centromere region of Cre-expressing *Mis18α*$^{f/\Delta}$ MEFs indicating an increase in the portion of *Mae*II- or *Hpa*II-sensitive demethylated DNA, leading to the fragmentation of centromeric DNA (Fig. II-25A). Otherwise, both DNA methylation-specific enzyme assay and bisulfite sequencing experiment confirmed that there were little or no changes for DNA repeat sequence regions (LINE-1), subtelomeric region (Chr.19), and euchromatic region (β-actin) in WT and Mis18α KO cells (Fig. II-25B and II-25C).

To prove the causal relationship between Mis18α deficiency and reduced centromeric DNA methylation, the methylation status was checked in *Mis18α*$^{\Delta/\Delta}$ MEFs reconstituted with Mis18αWT or Mis18α5LA. The methylation level of centromeric DNA in WT reconstituted *Mis18α*$^{\Delta/\Delta}$ MEFs was almost comparable to that of *Mis18α*$^{f/\Delta}$ MEFs, whereas Mis18α5LA failed to rescue the reduced methylation of centromeric DNA in *Mis18α*$^{\Delta/\Delta}$ MEFs (Fig. II-26A), confirming that the interaction between Mis18α and DNMT3A/3B is critical for maintaining the methylation status of centromeric DNA. Next it was tested whether centromeric transcript levels could be rescued by Mis18αWT or Mis18α5LA. In contrast to WT, 5LA mutant could not

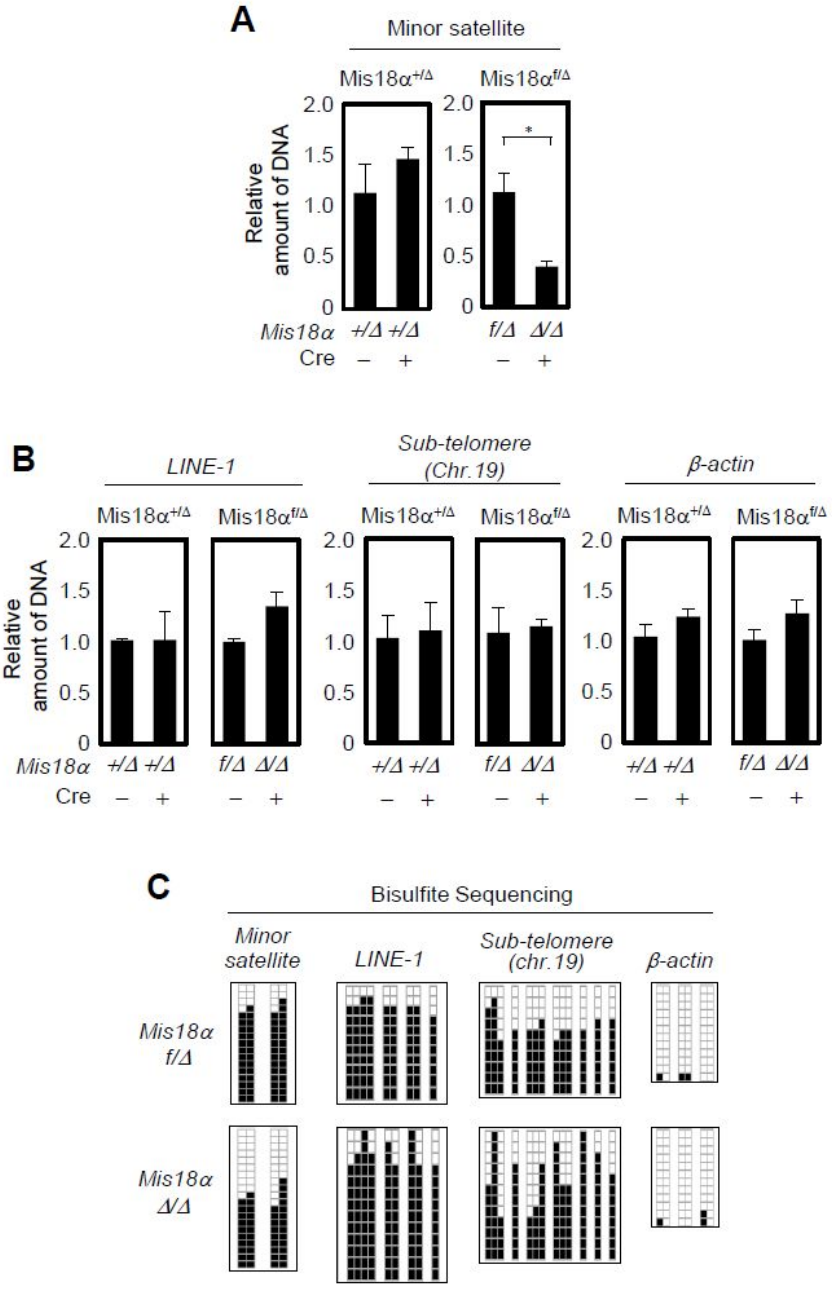
A
Minor satellite
Mis18α+/Δ
Mis18αf/Δ
Relative amount of DNA
2.0
1.5
1.0
0.5
0
*
Mis18α +/Δ +/Δ f/Δ Δ/Δ
Cre – + – +
B
LINE-1
Sub-telomere (Chr.19)
β-actin
Mis18α+/Δ
Mis18αf/Δ
Relative amount of DNA
Mis18α +/Δ +/Δ f/Δ Δ/Δ
Cre – + – + – + – + – + – +
C
Bisulfite Sequencing
Minor satellite
LINE-1
Sub-telomere (chr.19)
β-actin
Mis18α f/Δ
Mis18α Δ/Δ

Figure II-25. Reduced DNA methylation in *Mis18α*-deficient MEFs

(A and B) Genomic DNAs from *Mis18α*$^{+/\Delta}$ and *Mis18α*$^{f/\Delta}$ MEFs with or without Cre-expression were digested by methylation sensitive restriction enzymes (*Mae*II or *Hpa*II) followed by quantitative PCR using primers against minor satellite (A), LINE-1, Sub-telomere (Chr.19) and β-actin promoter regions (B). The values in (A) and (B) are expressed as mean ± SEM of three independent experiments. ∗ : $p < 0.05$, ∗∗ : $p < 0.01$. (C) Bisulfite genomic sequencing of minor satellite, LINE-1, Sub-telomere (Chr.19) and β-actin promoter regions in the *Mis18α*$^{f/\Delta}$ MEFs with or without Cre-expression. Black or white squares represent methylated or unmethylated CpG sites, respectively.

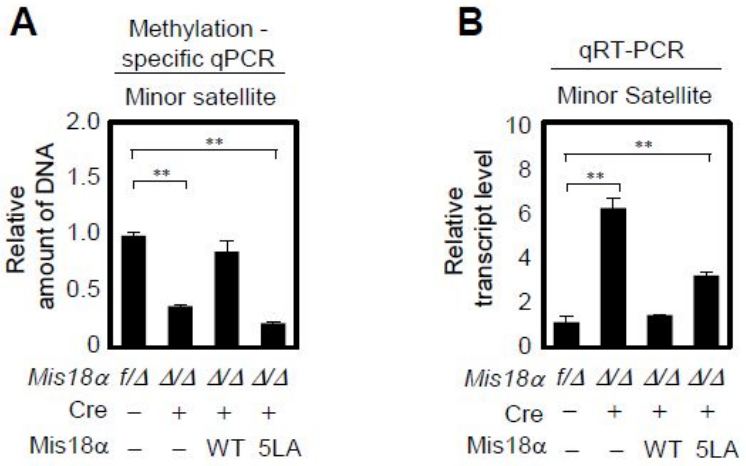

Figure II-26. 5LA Mutant of Mis18α Could Not Rescue DNA Methylation Level of Centromere.

(A) DNA methylation status in centromere region of *Mis18α*$^{f/\Delta}$ MEFs reconstituted with WT or 5LA with Cre-expression was examined using methylation sensitive restriction enzymes (*Mae*II or *Hpa*II) followed by quantitative PCR. (B) Quantitative RT-PCR was performed to define noncoding transcript levels from centromere region of MEFs used in (A).

reduce the increased transcripts level in *Mis18α*$^{\Delta/\Delta}$ MEFs to the level of *Mis18α*$^{f/\Delta}$ MEFs (Fig. II-26B). Taken together, these data indicate that reduced centromeric localization of DNMT3A/3B in *Mis18α*$^{\Delta/\Delta}$ MEFs led to the reduction of DNA methylation in centromere resulting in increased production of noncoding transcripts.

Based on the hypomethylation status of centromeric DNAs in *Mis18α*$^{\Delta/\Delta}$ MEFs, it was tested whether induced hypomethylation by knocking down of DNMT3A/B could abolish CENP-A loading. The numbers of cells exhibiting CENP-A dots were decreased to around 40 % in HeLa cells when DNMT3A/3B levels were reduced (Fig. II-27A). The centromeric localization of CENP-A was significantly reduced when DNMT3A/3B were depleted by siRNAs, which was comparable to the level of reduction by CENP-A knockdown (Fig. II-27B, left side histogram). On the other hand, the enrichment of DNMT3A/3B in centromere region was not affected by depletion of CENP-A (Fig. II-27B, right side histogram). These results were also confirmed in human cells (Fig. II-27C). Therefore, CENP-A loss in *Mis18α*$^{\Delta/\Delta}$ MEFs is directly mediated by reduced localization of DNMT3A/3B in centromere. Taken together, these studies demonstrate that DNMT3A/3B-mediated DNA methylation in centromere is a prerequisite for the centromeric localization of CENP-A and Mis18α plays a critical role in positioning DNMT3A/3B at centromere at specific cell stages.

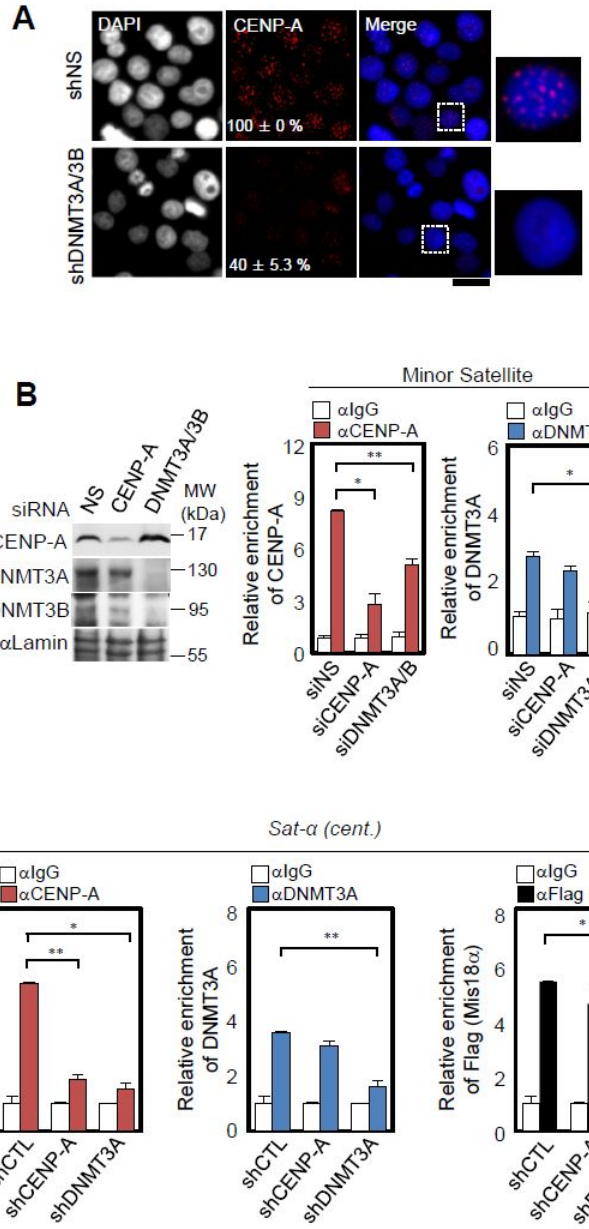
A
DAPI
CENP-A
Merge
shNS
100 ± 0 %
shDNMT3A/3B
40 ± 5.3 %
B
siRNA
NS
CENP-A
DNMT3A/3B
MW (kDa)
αCENP-A
αDNMT3A
αDNMT3B
αLamin
17
130
95
55
Minor Satellite
αIgG
αCENP-A
Relative enrichment of CENP-A
siNS
siCENP-A
siDNMT3A/B
αDNMT3A
Relative enrichment of DNMT3A
C
Sat-α (cent.)
αFlag (Mis18α)
Relative enrichment of Flag (Mis18α)
shCTL
shCENP-A
shDNMT3A

Figure II-27. Reduced DNA methylation is linked to the loss of CENP-A
(**A**) Immunocytochemistry was performed in HeLa cells transfected with indicated shRNAs. The percentage of cells showing CENP-A dots (red) was calculated by counting 400 cells. The insets are magnified to the right side. Scale bar: 20 μm. (B) ChIP assays were performed in *Mis18α*$^{f/\Delta}$ MEFs transfected with nonspecific siRNA or mixed siRNAs for Dnmt3a and Dnmt3b. Centromere occupancy by CENP-A was analyzed. (C) ChIP assays were performed in HeLa cells transfected with nonspecific shRNA or mixed shRNAs for DNMT3A and DNMT3B. Centromere occupancy by CENP-A was analyzed.

II-4. Discussion

The present approach to elucidate the physiological role of Mis18α using conditional knockout mouse first revealed its pivotal role in early embryonic development. Although Mis18α did not interact with CENP-A, *Mis18α*-deficiency led to loss of centromeric CENP-A and mitotic defects, suggesting that keeping centromeric localization of Mis18α is important to CENP-A loading and chromosome segregation. Interestingly, *Cenp-a*$^{-/-}$ mice failed to survive beyond E6.5 with severe mitotic problems including micro- and macro-nuclei, nuclear bridges, and chromatin fragmentation (Howman et al., 2000). In comparison with other centromere proteins, such as *Cenp-c* or *Incenp*, severe phenotype of embryos was slightly delayed in cenp-a knockout. Interestingly, *Mis18α*$^{\Delta/\Delta}$ embryo exhibited almost identical defects to *Cenp-a*$^{-/-}$ embryo. *Mis18α*$^{\Delta/\Delta}$ blastocysts developed severe chromosomal missegregation with lack of centromeric CENP-A resulting in cell death, and failed to grow in *in vitro* culture. Further, *Mis18α*$^{\Delta/\Delta}$ mice showed embryo lethality after E3.5 as *Cenp-a* knockout mice did. Although *Cenp-a* or *Mis18α* were prerequisites for cell division, *Cenp-a* or *Mis18α* knockout embryo survived and passed through numerous cell divisions until blastocyst stage. These results suggested that maternally derived Cenp-a or Mis18α proteins in oocyte substituted for the loss of the proteins in knockout embryo until the remaining maternally derived proteins were degraded in

blastocyst stage. The phenotypic similarity between these knockout mice supports the functional link between CENP-A and Mis18α. In addition, the analysis of Mis18α-deficient MEFs with the conditional deletion of the gene allowed us to elucidate that the functional role of Mis18α is required in general cell cycle stages.

I revealed that Mis18α complex including DNMT3A/3B plays a pivotal role in establishing centromeric chromatin states by modulating DNA methylation and histone modification in centromeric chromatins (Fig. II-28). Specific chromatin signatures exemplified by DNA methylation and histone modification are inherited to the daughter DNA strand during cell divisions (Moazed, 2011). CENP-A is also deposited to the centromere of daughter DNA strand from late mitosis to early G1 phase of cell cycle by the priming or licensing activity of Mis18α (Jansen et al., 2007; Probst et al., 2009). Altered centromeric chromatin states in *Mis18α*$^{\Delta/\Delta}$ MEFs suggested that licensing activity of Mis18α is necessary for establishing centromeric chromatin states including histone modifications such as H3K9me3, H3K4me2 or H3Ac. Although *Mis18α*$^{\Delta/\Delta}$ MEFs exhibited decreased recruitment of histone and DNA modifying enzymes in centromeric chromatin region, interestingly, DNMT3A/3B were identified as the sole interacting partners of Mis18α among histone and DNA modifying enzymes. These results speculated that altered histone modifications in the centromere region of *Mis18α*$^{\Delta/\Delta}$ MEFs might be due to the altered DNA methylation, based on the functional link between DNMTs and histone modifying enzymes (Cedar and Bergman, 2009; Fuks et al., 2003; Lehnertz et al., 2003; Ling et al., 2004).

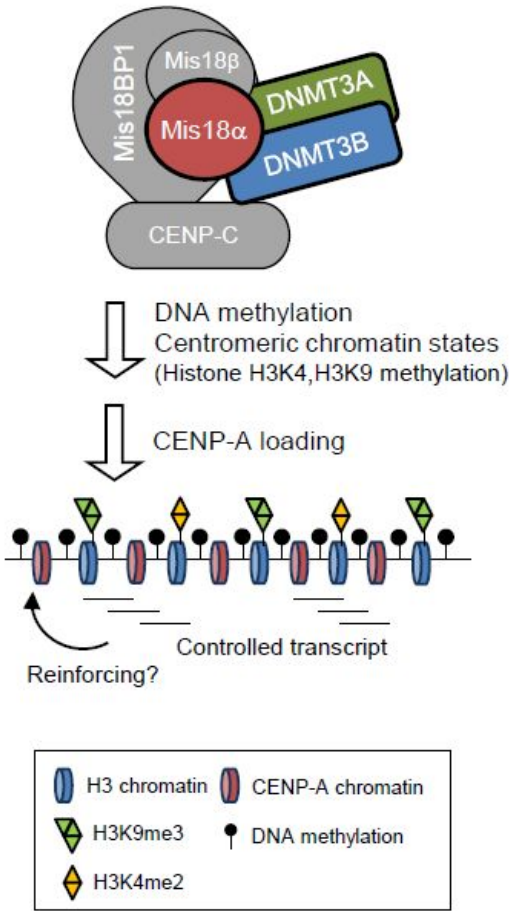

Figure II-28. A schematic model of regulation of CENP-A loading by Mis18α/DNMT3A/3B complex mediated centromeric DNA methylation.

A schematic diagram illustrating the proposed working mechanism of Mis18α. During late Mitosis to early G1, Mis18 complex are loaded in centromere region and interacts with CCAN proteins including CENP-C. This process facilitates centromeric enrichment of DNMT3A/3B and establishes centromeric DNA methylation status, providing a platform to recruit histone and DNA modifying enzymes responsible for epigenetic modulation of centromeric chromatin for CENP-A loading.

DNMT3B has been identified as a responsible enzyme for the methylation of minor satellite repeats in mouse ES cells and embryos (Okano et al., 1999). *DNMT3B* is a causal gene for immunodeficiency, centromere region instability, and facial anomalies (ICF) syndrome, exhibiting cellular properties such as hypomethylation of DNA at centric and pericentric regions, chromosome decondensation, anaphase bridge, and lagging chromosome during cell cycle (Ehrlich et al., 2008). These ChIP assays revealed that DNMT3A/3B were recruited to the centromeric chromatin region that overlaps with the Mis18α localization in a cell cycle-dependent manner. Lack of interaction between Mis18α and DNMT3A/3B led to the reduced DNA methylation in centromere. Further, knockdown of DNMT3A/3B resulted in reduced centromere localization of CENP-A. Therefore, Mis18α reinforces centromeric localization of DNMT3A/3B during mitosis to early G1 and hence provides the means to establish centromeric chromatin states for CENP-A loading. Recently, it has been reported that a constitutive centromere protein CENP-C recruits DNMT3B to centromere region and modulates DNA and histone methylation (Gopalakrishnan et al., 2009). The loss of CENP-C or DNMT3B led to chromosome segregation defects during mitosis, elevated transcription of centromeric repeats, and alteration of histone methylation patterns, which are similar to the defects in *Mis18α*$^{\Delta/\Delta}$ MEFs. In addition, depletion of CENP-C using CENP-C specific antibody disrupted centromeric localization of Mis18BP1, a component of Mis18α complex (Moree et al., 2011). Although CENP-C conducts an important role in centromeric localization of Mis18 complex by binding to

DNMT3A/3B and Mis18BP1, these data suggest that the interaction between Mis18α and DNMT3A/3B appears to be CENP-C-independent. The integrity of stable Mis18 complex consisting of Mis18α/Mis18β/Mis18BP1/ CENP-C/DNMT3A/3B formed at centromere provide the plausible explanation why knockdown of either Mis18α or DNMT3A/3B impairs centromeric localization of Mis18 complex. I speculate that Mis18α and DNMT3A/3B reinforce each other's function by reciprocally regulating stability of Mis18 complex at centromere.

Given that increased noncoding transcripts alter centromere architecture and function (Bouzinba-Segard et al., 2006), reduced DNA and histone methylation with elevated noncoding transcripts contributes to altered centromere architecture in *Mis18α*$^{\Delta/\Delta}$ MEFs. In the absence of Mis18α, reduced level of DNMT3A/3B at centromere is not sufficient for maintaining DNA methylation in sister centromere during cell division, which leads to uncontrolled accumulation of noncoding transcripts from centromere. These altered transcripts might disturb recruitment of protein complex responsible for re-establishing centromeric chromatin states. Therefore, altered centromeric chromatin states in *Mis18α*$^{\Delta/\Delta}$ are not suitable for loading nascent CENP-A on centromere. Thus, Mis18α/DNMT3A/3B complex could establish the methylation status on centromeric DNA and the proper chromatin states of centromere during mitosis to early G1 for CENP-A loading.

The CENP-A loading defects upon deletion of Mis18α was mediated not only by altered heterochromatin states (H3K9me2/me3 and DNA methylation) but also by

altered euchromatin states, such as H3K4me2. This discrepancy could be explained by a recent report stating that malfunction of artificial kinetochore was mediated by induced heterochromatin states in centromere as well as by induced euchromatin states (Nakano et al., 2008). *Mis18α*-deficiency might disrupt this balanced regulation between heterochromatin and euchromatin states in centromeric chromatin, which is required for centromere function. Further, demethylation of centromeric H3K4me2 by the demethylating enzyme LSD1 has been shown to interfere with CENP-A incorporation and also HJURP recruitment (Bergmann et al., 2011). In view of reduced centromeric H3K4me2 level in *Mis18α*$^{\Delta/\Delta}$ MEFs, defective centromeric chromatin states by deletion of Mis18α might lead to the impaired CENP-A loading and also reduced recruitment of HJURP in centromere. This possibility was supported by recent data that siRNA against Mis18α eliminated HJURP recruitment to centromere (Barnhart et al., 2011).

CENP-A deposition in higher eukaryotes is not determined by DNA sequence but rather by inherited centromeric chromatins. During cell division, chromatin modification and DNA methylation of centromere region should be properly inherited to sister centromere by protein complexes establishing histone or DNA methylation. These findings demonstrate that Mis18α plays a role in establishing DNA methylation and noncoding transcripts in centromere by interacting with DNMT3A/3B. Therefore, Mis18α functions as a licensing factor for CENP-A loading is in propagating centromere identity.

II-5. Materials and Methods

Generation of conditional Mis18α knockout mice, genotyping, and breeding

To create a conditional targeting vector in which exons 1 and 2 of the *Mis18α* gene was flanked by *loxP* sites, a 10.5 kb region used to construct the targeting vector was first sub-cloned from a positively identified C57BL/6 BAC clone (RPCI-23) into a pSP72 backbone vector (Promega). The region was designed such that the short homology arm extends about 1.5 kb 3' to exon 2. The long homology arm ends 5' to exon 1 and is ~6.5 kb long. The *loxP* flanked Neo cassette from a pGK-gb2 loxP/FRT-Neo was inserted on the 3' side of exon 2 and the single loxP site is inserted at the 5' side of exon 1. The target region was ~2.5 kb and included exons 1 and 2. The total size of the targeting construct including vector backbone and Neo cassette was 14.7 kb. Ten micrograms of the targeting vector was linearized by *Cla*I and then transfected by electroporation of C57BL/6 embryonic stem cells. After selection in G418 antibiotic, surviving clones were expanded to identify recombinant ES clones by Southern blot analysis. For *Eco*RI digestion, the bands representing wild-type and mutant alleles are 8.4 and 6.6 kb, respectively. Targeted ES cells were microinjected into Balb/c blastocysts which were in turn used to generate chimeras. The male chimeras were mated to C57BL/6 female mice to obtain F1 heterozygous offspring. Tail DNA samples from F1 mice were amplified by PCR using a primer pair (SDL1: 5'-CTCCGTTCCGTCTTGGCACAC-3', LOX1: 5'-CCTAAGTCGTTGACCTGACCGA

GG-3') to identify gene targeted F1 mice. *Neo* selection cassette or floxed exons were deleted by crossing targeted heterozygous F1 with a Flp deleter strain (FLPeR mice, The Jackson Laboratory strain 003946) or with *protamine-Cre* mice (The Jackson Laboratory strain 003328), respectively. All mice used for this work were backcrossed to C57BL/6 at least five generations. All mice were handled in accordance with guidelines of Seoul National University or Sookmyung Women's University, and procedures were approved by the Institutional Animal Care and Use Committee of each university.

***In vitro* culture, immunostaining, and TUNEL assay of pre-implantation embryos**

Detailed conditions for the experiments were described previously (Jeon et al., 2011). E3.5 blastocysts were obtained from *Mis18α*$^{+/\Delta}$ females that were crossed with heterozygous males. For the outgrowth assays, blastocysts were cultured *in vitro*, photographed daily, and harvested at the end of experiment for genotyping. The primary antibodies used for immunostaining were rabbit anti-phosphohistone H3 (Ser-10) (Cell Signaling), mouse anti-α-tubulin (Calbiochem), and rabbit anti-CENP-A (Abcam). The TUNEL (Terminal deoxynucleotidyltransferase-mediated dUTP-biotin nick end labeling) assay was performed according to the manufacturer's instructions (Roche).

MEF generation and Cre-retrovirus infection

MEFs were generated as previously described (Kim et al., 2006; Lee et al., 2006). To obtain Cre expressing retrovirus, stable virus-producing cell line was generated. PT67 packaging cells (Clonetech) transfected with retroviral plasmid expressing Cre recombinase were grown in puromycin selection media and the clone producing high titer virus particle (PT67-Cre) was obtained. Culture supernatants containing PT67-Cre were harvested, filtered, and used for infection. *Mis18α*$^{+/\Delta}$ or *Mis18α*$^{f/\Delta}$ MEFs were incubated with virus for 4 hr in the presence of 8 μg/ml polybrene (Sigma). Cells were treated with 3 μg/ml of puromycin for 48 hr for selection.

Immunocytochemistry

The cells grown on coverslips were washed three times with PBS and then fixed with 2% paraformaldehyde in PBS for 10 min at room temperature. Fixed cells were permeabilized with 0.5% Triton X-100 in PBS (PBS-T) for 10 min at room temperature. Blocking was performed with 3% bovine serum and 10% gelatin in PBS-T for 30 min. For staining, cells were incubated with affinity-purified anti-Flag IgG overnight at 4°C, followed by incubation with fluorescent labeled secondary antibodies for 1 hr at room temperature (Invitrogen).

Chromosome spreading assay

MEFs or HeLa cells were arrested at mitosis by incubating with 2 μg/ml nocodazole for 12 hr. Arrested cells were collected by shaking off, washed with PBS, and incubated in hypotonic solution (75 mM KCl) for 10 min. Cells were spreaded onto slides using Cytospin (Thermo Scientific) by spinning at 1,000 rpm for 5 min, and fixed with 4% paraformaldehyde in PBS for 15 min. CENP-A protein was visualized by immunofluorescence.

Cell cycle synchronization

Cell cycle of HeLa and MEFs were arrested at G1/S by double thymidine block. Cells were incubated with media containing 2 mM thymidine for 16 hr, washed twice with PBS, and cultured in complete media for 9 hr. Cells were again incubated with thymidine containing media for 12 hr followed by washing and culturing in normal media. Cells were harvested at indicated time points for experiment. Transfected cells were incubated with first thymidine media a day after transfection.

ChIP, Sequential-ChIP, and qPCR

The ChIP and two-step ChIP assays were conducted as previously described (Baek et al., 2002; Kim et al., 2005). Quantitative PCR (qPCR) was used to measure enrichment of bound DNA and the value of enrichment was calculated by relative amount to input and ratio to IgG. The PCR conditions were 95°C (5 min) and 40 cycles of 95°C (30 s), 57°C (30 s), and 72°C (30 s). All reactions were performed in

triplicates. The primers used in ChIP assay were listed in the Supplementary Information. The following primers were used: minor satellite repeats forward 5'-CATGGAAAATGATAAAAACC-3', reverse 5'-CATCTAATATGTTCTACAGTG TGG-3' (Lehnertz et al., 2003) ; satellite α (satα) repeats forward 5'-CTGCACTACCTGAAGAGGAC-3', reverse 5'-GATGG TTCAACACTCTTACA-3' (Gopalakrishnan et al., 2009) ; promoter region of β-actin forward 5'-TCGAT ATCCACGTGACATCCA-3', reverse 5'-GCAGCATTTTTTTACCCCCTC-3'; promoter region of GAPDH forward 5'-AGAGAGGGAGGAGGGGAAATG-3', reverse 5'-CAGGGAGGAGCAGAGAGCAC-3'; LINE-1 forward 5'-AATGGCTT GTGCTGTAAGAT CG-3', reverse 5'-AATCTGTTGGTGGTCTTTTTGTC-3' ; IAP1 forward 5'-CACGCTCCGG TAGAATACTTAC-3', reverse 5'-GCCATGCCGG CGAGCCTGT-3'; sub-telomere (Chr.19) forward 5'-TTTTTCTTGCTGGAC GAGGT-3', reverse 5'-ACAAAAGCAGAGGCC AGAAA-3'.

DNA methylation analysis

Methylation status in satellite repeat regions was analyzed by methylation-sensitive restriction enzyme and bisulfate sequencing. The genomic DNAs extracted from *Mis18α*$^{+/\Delta}$ or *Mis18α*$^{f/\Delta}$ MEFs were digested with *Mae*II or *Hpa*II. After digestion, the amounts of undigested DNAs were analyzed by quantitative PCR using satellite repeat primers as in ChIP assay. The bisulfite modification of genomic DNA was performed using EZ DNA Methylation-Gold kit according to manufacturer's

instructions (Zymo research). For sequencing, 20 colonies were obtained and analyzed to determine methylated CpG sites in each region. The primer sequences are listed in the Supplementary Information. The following primers were designed by online tools, MethPrimer: minor satellite repeat forward 5'-TAGAATATATTAGAT GAGTGAGTTATATTG-3', reverse 5'-ATTATAACTCATTAATATACACTATTCT AC-3'; LINE-1 forward 5'-GTTAGAGAATTTGATAGTTTTTGGAATAGG-3', reverse 5'-CCAAAACAAAACCTTTCTCAAACACTATAT-3'; Sub-telomere (Chr.19) forward 5'-TAGTGTTGGGGTGTATATAAGTAGT-3', reverse 5'-CTAACCAACC TTAACTACTTCTATC-3';; promoter region of β-actin forward 5'-AATTGTTAGT AAGGGGGAGTGAT TT-3', reverse 5'-CACCCCAAAACCCTCTAAATATAA-3'

Antibodies

The following antibodies were purchased from Abcam; anti-CENP-A, CENP-C, DNMT3A, DNMT3B, HP1β, H3K9me3, and Histone H3. Other antibodies used were anti-α-tubulin and anti-FLAG (Sigma), anti-HA (Covance), anti-HP1α, anti-H3K9me2 and phospho-H3S10 (Cell Signaling), anti-H3Ac (Millipore), and anti-G9a, anti-GLP and anti-SUV39H1 (Upstate Biotechnology). Anti-mouse Mis18α antibody was generated by injecting 6His-tagged mouse Mis18α protein to rabbit (Abfrontier, South Korea).

Plasmid Construction

Deletion mutants of Mis18α, DL1 (38-204 aa), DL2 (119-204 aa), DL3 (1-135 aa), ΔLRR (1-182 aa) were amplified by PCR using primers corresponding to each mutation. The amplified fragments were digested with *EcoR*I and *Kpn*I and ligated to pCMV10 plasmid vector digested with the same enzymes. Mis18α5LA mutant was generated by site-directed mutagenesis using nPfu-Forte DNA polymerase (Enzynomics, South Korea) and by repeating mutagenesis step twice. For fusion protein, PCR amplified Mis18α or 5LA mutant was fused to C-terminus of Mis18β. All mutants were verified by sequencing.

FACS analysis

Cultured cells were fixed in 70% ethanol and stained with propidium iodide staining solution (20 μg/ml propidium iodide, 200 μg/ml DNase-free RNase A, and 0.1% Triton X-100 in PBS). Cell cycle and DNA contents were analyzed using a FACS Caliber flow cytometer and CellQuest software (BD Biosciences).

RNA interference by siRNA and shRNA

For knockdown of specific genes, cells were transfected with siRNA or shRNA as indicated in figures and harvested for experiments 72 hr after transfection. The target sequences of shRNA or siRNA against endogenous CENP-A, DNMT3A and DNMT3B are as follows: siCENP-A (mouse), 5'-GAGAAAUAUGUGAGAAGUU-

3’; siDNMT3A (mouse) and shDNMT3A (human), 5’-GGCUGUGGAAGU GCAGAACUU-3’; siDNMT3B (mouse), 5’-GUAGAUGA UGGGAAUGGCUUU-3’; shDNMT3B (human), 5’-GGGCUUCUCCUGGUGGCCU-3’; and siNS, 5’-CUGGACUUCCAGAAGAACAUC-3’.

Measuring noncoding transcripts from satellite repeat regions

Total RNA was prepared from MEFs using RNAeasy kit according to the manufacturer’s instructions (Qiagen). Transcript level was analyzed by quantitative RT-PCR with satellite specific primers as in ChIP assay. The quantity of transcripts was calculated using the ΔΔCt method and normalized by comparing to GAPDH. All reactions were performed in triplicates.

Statistical analysis

Statistical differences in test and control samples were determined by student’s t-test using the Statview package (Abacus Concepts, Inc., Berkeley, CA).

CHAPTER III

Conclusion

During cell division, the centromere is defined and maintained by chromatin structure composed of CENP-A. Mis18α has been shown to regulate CENP-A deposition by localizing at the centromere from late mitosis to early G1 phase, which occurs slightly ahead of CENP-A loading. This process ensures CENP-A to specify centromere identity. Although this 'licensing' or 'priming' function of Mis18α is required for the localization of CENP-A at centromere, the mechanisms underlying CENP-A deposition have been unidentified. In this study, *Mis18α*-deficient mouse revealed that Mis18α-mediated CENP-A loading is crucial for embryonic development, especially during cell division. Licensing function of Mis18α by interacting with DNMT3A/3B reinforced their centromeric localization and hence preserved epigenetic status including DNA methylation which represents epigenetic states of the cells, to ensure CENP-A loading.

Embryos from conditional knockout mice for *Mis18α* stopped growing after blastocyst stages and died around embryonic day 3.5. Knockout embryo showed severe defects of chromosome segregation including satellite chromosome, anaphase bridges and altered metaphase alignments and lack of CENP-A in centromere. Interestingly, the phenotypes observed in knockout embryo were identical to phenotypes of *Cenp-a* knockout embryo, suggesting that severe mitotic defects were caused by the loss of CENP-A loading. To verify the consequence of mitotic defects, blastocysts were cultured *in vitro* and their cell growth was monitored in development. Knockout embryo showed growth retardation and disappearance of inner cell mass at

later stages due to cell death. This cell death was confirmed by TUNEL assay, indicating that accumulation of missegregattion by loss of CENP-A in *Mis18α*-deficient embryo led to apoptotic cell death. Consistent with the results in embryos, *Mis18α*$^{\Delta/\Delta}$ MEFs that were generated by Cre introduction showed loss of CENP-A loading and altered chromosome segregation. DNA damage and apoptosis were also observed in knockout MEFs. Taken together, *Mis18α*-deficiency led to the loss of CENP-A at centromere and missegregation of chromosome during cell division. Therefore, *Mis18α*-deficient embryos were lethal in early embryonic development by mitotic defects-mediated apoptosis.

In general, centromere shows distinct characteristics of chromatin, including both of euchromatic and heterochromatic states, such as H3K4me2 or H3Ac and H3K9me3, respectively. These chromatin states were altered in *Mis18α*$^{\Delta/\Delta}$ MEFs, suggesting that the 'licensing' function of Mis18α is to maintain epigenetic states of centromere. Further, centromeric noncoding transcripts which were tightly regulated by centromere specific chromatin states were increased in knockout MEFs. In the screening of proteins that participate in maintenance of centromeric chromatin states, DNMT3A and DNMT3B were identified as Mis18α-interacting proteins. Centromeric localization of DNMT3A/3B was reduced in *Mis18α*$^{\Delta/\Delta}$ MEFs and that of Mis18α was reduced by knockdown of DNMT3A/3B. This mutual reinforcement of localization suggests that centromeric DNA methylation is spatially and temporally maintained by cooperation between them. Bisulfite sequencing revealed that

hypomethylation of DNA in *Mis18α*$^{\Delta/\Delta}$ MEFs was observed only in centromere and this hypomethylation was reversed by reconstituting with Mis18α. Thus, 'licensing' function of Mis18α was obtained by its interaction with DNMT3A/3B whose role is to maintain DNA methylation in centromere. Therefore, controlled DNA methylation in centromere is required for centromeric localization of CENP-A during mitosis.

Taken together, these results show that CENP-A deposition during cell division is mediated through modulating of centromeric chromatin, especially centromeric DNA methylation which is regulated by Mis18α/DNMT3A/3B complex. Mitosis-specific localization of this complex ensures their enrichment on centromere and centromeric DNA methylation in daughter cells. Epigenetic regulation of centromere by Mis18α to maintain CENP-A loading supports functional role of Mis18α to retain centromeric identity.

REFERENCES

Allshire, R.C., and Karpen, G.H. (2008). Epigenetic regulation of centromeric chromatin: old dogs, new tricks? Nat. Rev. Genet. *9*, 923-937.

Allshire, R.C., Nimmo, E.R., Ekwall, K., Javerzat, J.P., and Cranston, G. (1995). Mutations derepressing silent centromeric domains in fission yeast disrupt chromosome segregation. Genes Dev. *9*, 218-233.

Amor, D.J., and Choo, K.H.A. (2002). Neocentromeres: role in human disease, evolution, and centromere study. Am. J. hum. Genet. *71*, 695-714.

Amor, D.J., Kalitsis, P., Sumer, H., and Andy Choo, K.H. (2004). Building the centromere: from foundation proteins to 3D organization. Trends Cell Biol. *14*, 359-368.

Ando, S., Yang, H., Nozaki, N., Okazaki, T., and Yoda, K. (2002). CENP-A, -B, and -C chromatin complex that contains the I-Type α-Satellite array constitutes the prekinetochore in HeLa cells. Mol. Cell. Biol. *22*, 2229-2241.

Baek, S.H., Ohgi, K.A., Rose, D.W., Koo, E.H., Glass, C.K., and Rosenfeld, M.G. (2002). Exchange of N-CoR corepressor and Tip60 coactivator complexes links gene expression by NF-κB and beta-amyloid precursor protein. Cell *110*, 55-67.

Barnhart, M.C., Kuich, P.H.J.L., Stellfox, M.E., Ward, J.A., Bassett, E.A., Black, B.E., and Foltz, D.R. (2011). HJURP is a CENP-A chromatin assembly factor sufficient to form a functional de novo kinetochore. J. Cell Biol. *194*, 229-243.

Bergmann, J.H., Rodriguez, M.G., Martins, N.M.C., Kimura, H., Kelly, D.A., Masumoto, H., Larionov, V., Jansen, L.E.T., and Earnshaw, W.C. (2011). Epigenetic engineering shows H3K4me2 is required for HJURP targeting and CENP-A assembly on a synthetic human kinetochore. EMBO J *30*, 328-340.

Bernad, R., Sáncheza, P., and Losada, A. (2009). Epigenetic specification of centromeres by CENP-A. Exp. Cell Res. *315*, 3233-3241.

Bernad, R., Sáncheza, P., Rivera, T., Rodríguez-Corsino, M., Boyarchuk, E., Vassias, I., Ray-Gallet, D., Arnaoutov, A., Dasso, M., Almouzni, G*., et al.* (2011). Xenopus HJURP and condensin II are required for CENP-A assembly. J. Cell Biol. *192*, 569-582.

Black, B.E., and Bassett, E.A. (2008). The histone variant CENP-A and centromere specification. Curr. Opin. Cell Biol. *20*, 91-100.

Black, B.E., Brock, M.A., Bédard, S., Woods, V.L., and Cleveland, D.W. (2007a). An epigenetic mark generated by the incorporation of CENP-A into centromeric nucleosomes. Proc. Natl. Acad. Sci. *104*, 5008-5013.

Black, B.E., Foltz, D.R., Chakravarthy, S., Luger, K., Woods, V.L., and Cleveland, D.W. (2004). Structural determinants for generating centromeric chromatin. Nature *430*, 578-582.

Black, B.E., Jansen, L.E.T., Maddox, P.S., Foltz, D.R., Desai, A.B., Shah, J.V., and Cleveland, D.W. (2007b). Centromere identity maintained by nucleosomes assembled with histone H3 containing the CENP-A targeting domain. Mol. Cell *25*, 309-322.

Blower, M.D., Sullivan, B.A., and Karpen, G.H. (2002). Conserved organization of centromeric chromatin in flies and humans. Dev. Cell *2*, 319-330.

Bouzinba-Segard, H., Guais, A., and Francastel, C. (2006). Accumulation of small murine minor satellite transcripts leads to impaired centromeric architecture and function. Proc. Natl. Acad. Sci. *103*, 8709-8714.

Carroll, C.W., Milks, K.J., and Straight, A.F. (2010). Dual recognition of CENP-A nucleosomes is required for centromere assembly. J. Cell Biol. *189*, 1143-1155.

Carroll, C.W., Silva, M.C.C., Godek, K.M., Jansen, L.E.T., and Straight, A.F. (2009). Centromere assembly requires the direct recognition of CENP-A nucleosomes by CENP-N. Nat. Cell Biol. *11*, 896-902.

Cedar, H., and Bergman, Y. (2009). Linking DNA methylation and histone modification: patterns and paradigms. Nat. Rev. Genet. *10*, 295-304.

Cheeseman, I.M., Drubin, D.G., and Barnes, G. (2002). Simple centromere, complex kinetochore. J. Cell Biol. *157*, 199-203.

Chen, T., Tsujimoto, N., and Li, E. (2004). The PWWP Domain of Dnmt3a and Dnmt3b Is Required for Directing DNA Methylation to the Major Satellite Repeats at Pericentric Heterochromatin. Mol. Cell. Biol. *24*, 9048-9058.

Chen, T., Ueda, Y., Dodge, J.E., Wang, Z., and Li, E. (2003). Establishment and maintenance of genomic methylation patterns in mouse embryonic stem cells by Dnmt3a and Dnmt3b. Mol. Cell. Biol. *23*, 5594-5605.

Cleveland, D.W., Mao, Y., and Sullivan, K.F. (2003). Centromeres and kinetochores: from epigenetics to mitotic checkpoint signaling. Cell *112*, 407-421.

Craig, J.M., Earle, E., Canham, P., Wong, L.H., Anderson, M., and Choo, K.H.A. (2003). Analysis of mammalian proteins involved in chromatin modification reveals new metaphase centromeric proteins and distinct chromosomal distribution patterns. Hum. Mol. Genet. *12*, 3109-3121.

Dunleavy, E.M., Roche, D., Tagami, H., Lacoste, N., Ray-Gallet, D., Nakamura, Y., Daigo, Y., Nakatani, Y., and Almouzni-Pettinotti, G. (2009). HJURP is a cell-cycle-dependent maintenance and deposition factor of CENP-A at centromeres. Cell *137*, 485-497.

Ehrlich, M., Sanchez, C., Shao, C., Nishiyama, R., Kehrl, J., Kuick, R., Kubota, T., and Hanash, S.M. (2008). ICF, an immunodeficiency syndrome: DNA methyltransferase 3B involvement, chromosome anomalies, and gene dysregulation. Autoimmunity *41*, 253-271.

Fitzgerald-Hayes, M., Clarke, L., and Carbon, J. (1982). Nucleotide sequence comparisons and functional analysis of yeast centromere DNAs. Cell *29*, 235-244.

Folco, H.D., Pidoux, A.L., Urano, T., and Allshire, R.C. (2008). Heterochromatin and RNAi are required to establish CENP-A chromatin at centromeres. Science *319*, 94-97.

Foltz, D.R., Jansen, L.E.T., Bailey, A.O., Yates Iii, J.R., Bassett, E.A., Wood, S., Black, B.E., and Cleveland, D.W. (2009). Centromere-specific assembly of CENP-A nucleosomes is mediated by HJURP. Cell *137*, 472-484.

Foltz, D.R., Jansen, L.E.T., Black, B.E., Bailey, A.O., Yates, J.R., and Cleveland, D.W.

(2006). The human CENP-A centromeric nucleosome-associated complex. Nat. Cell Biol. *8*, 458-469.

Fujita, Y., Hayashi, T., Kiyomitsu, T., Toyoda, Y., Kokubu, A., Obuse, C., and Yanagida, M. (2007). Priming of centromere for CENP-A recruitment by human hMis18α, hMis18β, and M18BP1. Dev. Cell *12*, 17-30.

Fukagawa, T., and Brown, W.R.A. (1997). Efficient conditional mutation of the vertebrate CENP-C gene. Hum. Mol. Genet. *6*, 2301-2308.

Fukagawa, T., Mikami, Y., Nishihashi, A., Regnier, V., Haraguchi, T., Hiraoka, Y., Sugata, N., Todokoro, K., Brown, W., and Ikemura, T. (2001). CENP-H, a constitutive centromere component, is required for centromere targeting of CENP-C in vertebrate cells. EMBO J *20*, 4603-4617.

Fuks, F., Hurd, P.J., Wolf, D., Nan, X., Bird, A.P., and Kouzarides, T. (2003). The methyl-CpG-binding protein MeCP2 links DNA methylation to histone methylation. J. Biol. Chem. *278*, 4035-4040.

Gopalakrishnan, S., Sullivan, B.A., Trazzi, S., Della Valle, G., and Robertson, K.D. (2009). DNMT3B interacts with constitutive centromere protein CENP-C to modulate DNA methylation and the histone code at centromeric regions. Hum. Mol. Genet. *18*, 3178-3193.

Grewal, S.I.S., and Jia, S. (2007). Heterochromatin revisited. Nat. Rev. Genet. *8*, 35-46.

Guenatri, M., Bailly, D., Maison, C., and Almouzni, G. (2004). Mouse centric and pericentric satellite repeats form distinct functional heterochromatin. J. Cell Biol. *166*, 493-505.

Hayashi, T., Fujita, Y., Iwasaki, O., Adachi, Y., Takahashi, K., and Yanagida, M. (2004). Mis16 and Mis18 are required for CENP-A loading and histone deacetylation at centromeres. Cell *118*, 715-729.

Heit, R., Underhill, D.A., Chan, G., and Hendzel, M.J. (2011). Epigenetic regulation of centromere formation and kinetochore function. Biochem. Cell Biol. *84*, 605-630.

Henikoff, S., Ahmad, K., and Malik, H.S. (2001). The centromere paradox: stable inheritance with rapidly evolving DNA. Science *293*, 1098-1102.

Howman, E.V., Fowler, K.J., Newson, A.J., Redward, S., MacDonald, A.C., Kalitsis, P., and Choo, K.H.A. (2000). Early disruption of centromeric chromatin organization in centromere protein A (Cenpa) null mice. Proc. Natl. Acad. Sci. *97*, 1148-1153.

Hudson, D.F., Fowler, K.J., Earle, E., Saffery, R., Kalitsis, P., Trowell, H., Hill, J., Wreford, N.G., de Kretser, D.M., Cancilla, M.R.*, et al.* (1998). Centromere protein B null mice are mitotically and meiotically normal but have lower body and testis weights. J. Cell Biol. *141*, 309-319.

Jansen, L.E.T., Black, B.E., Foltz, D.R., and Cleveland, D.W. (2007). Propagation of centromeric chromatin requires exit from mitosis. J. Cell Biol. *176*, 795-805.

Jeon, Y., Ko, E., Lee, K.Y., Ko, M.J., Park, S.Y., Kang, J., Jeon, C.H., Lee, H., and Hwang, D.S. (2011). TopBP1 deficiency causes an early embryonic lethality and induces cellular senescence in primary cells. J. Biol. Chem. *286*, 5414-5422.

Kalitsis, P., Fowler, K.J., Earle, E., Hill, J., and Choo, K.H.A. (1998). Targeted

disruption of mouse centromere protein C gene leads to mitotic disarray and early embryo death. Proc. Natl. Acad. Sci. *95*, 1136-1141.

Kim, J.H., Kim, B., Ling, C., Choi, H.J., Ohgi, K.A., Chen, C., Chung, C.H., Huber, O., Rose, D.W., Sawyers, C.L.*, et al.* (2005). Transcriptional regulation of a metastasis suppressor gene by Tip60 and beta-Catenin Complexes. Nature *434*, 921-926.

Kim, K.I., Yan, M., Malakhova, O., Luo, J.-K., Shen, M.-F., Zou, W., de la Torre, J.C., and Zhang, D.-E. (2006). Ube1L and protein ISGylation are not essential for alpha/beta interferon signaling. Mol. Cell. Biol. *26*, 472-479.

Kline-Smith, S.L., Sandall, S., and Desai, A. (2005). Kinetochore–spindle microtubule interactions during mitosis. Curr. Opin. Cell Biol. *17*, 35-46.

Kobe, B., and Kajava, A.V. (2001). The leucine-rich repeat as a protein recognition motif. Curr. Opin. Struct. Biol. *11*, 725-732.

Kwon, M.-S., Hori, T., Okada, M., and Fukagawa, T. (2007). CENP-C is involved in chromosome segregation, mitotic checkpoint function, and kinetochore assembly. Molecular Biology of the Cell *18*, 2155-2168.

Lagana, A., Dorn, J.F., De Rop, V., Ladouceur, A.-M., Maddox, A.S., and Maddox, P.S. (2010). A small GTPase molecular switch regulates epigenetic centromere maintenance by stabilizing newly incorporated CENP-A. Nat. Cell Biol. *12*, 1186-1193.

Lee, H., Lee, D.J., Oh, S.P., Park, H.D., Nam, H.H., Kim, J.M., and Lim, D.-S. (2006). Mouse emi1 has an essential function in mitotic progression during early

embryogenesis. Mol. Cell. Biol. *26*, 5373-5381.

Lehnertz, B., Ueda, Y., Derijck, A.A.H.A., Braunschweig, U., Perez-Burgos, L., Kubicek, S., Chen, T., Li, E., Jenuwein, T., and Peters, A.H.F.M. (2003). Suv39h-mediated histone H3 lysine 9 methylation directs DNA methylation to major satellite repeats at pericentric heterochromatin. Curr. Biol. *13*, 1192-1200.

Ling, Y., Sankpal, U.T., Robertson, A.K., McNally, J.G., Karpova, T., and Robertson, K.D. (2004). Modification of de novo DNA methyltransferase 3a (Dnmt3a) by SUMO-1 modulates its interaction with histone deacetylases (HDACs) and its capacity to repress transcription. Nucl. Acids Res. *32*, 598-610.

Lippman, Z., and Martienssen, R. (2004). The role of RNA interference in heterochromatic silencing. Nature *431*, 364-370.

Maddox, P.S., Hyndman, F., Monen, J., Oegema, K., and Desai, A. (2007). Functional genomics identifies a Myb domain-containing protein family required for assembly of CENP-A chromatin. J. Cell Biol. *176*, 757 -763.

Martens, J.H.A., O'Sullivan, R.J., Braunschweig, U., Opravil, S., Radolf, M., Steinlein, P., and Jenuwein, T. (2005). The profile of repeat-associated histone lysine methylation states in the mouse epigenome. EMBO J *24*, 800-812.

Moazed, D. (2011). Mechanisms for the inheritance of chromatin states. Cell *146*, 510-518.

Moree, B., Meyer, C.B., Fuller, C.J., and Straight, A.F. (2011). CENP-C recruits M18BP1 to centromeres to promote CENP-A chromatin assembly. J. Cell Biol. *194*, 855-871.

Nakano, M., Cardinale, S., Noskov, V.N., Gassmann, R., Vagnarelli, P., Kandels-Lewis, S., Larionov, V., Earnshaw, W.C., and Masumoto, H. (2008). Inactivation of a human kinetochore by specific targeting of chromatin modifiers. Dev. Cell *14*, 507-522.

Nishihashi, A., Haraguchi, T., Hiraoka, Y., Ikemura, T., Regnier, V., Dodson, H., Earnshaw, W.C., and Fukagawa, T. (2002). CENP-I is essential for centromere function in vertebrate cells. Dev. Cell *2*, 463-476.

Okada, M., Cheeseman, I.M., Hori, T., Okawa, K., McLeod, I.X., Yates, J.R., Desai, A., and Fukagawa, T. (2006). The CENP-H-I complex is required for the efficient incorporation of newly synthesized CENP-A into centromeres. Nat. Cell Biol. *8*, 446-457.

Okano, M., Bell, D.W., Haber, D.A., and Li, E. (1999). DNA methyltransferases Dnmt3a and Dnmt3b are essential for de novo methylation and mammalian development. Cell *99*, 247-257.

Palmer, D.K., O'Day, K., Trong, H.L., Charbonneau, H., and Margolis, R.L. (1991). Purification of the centromere-specific protein CENP-A and demonstration that it is a distinctive histone. Proc. Natl. Acad. Sci. *88*, 3734-3738.

Perez-Castro, A.V., Shamanski, F.L., Meneses, J.J., Lovato, T.L., Vogel, K.G., Moyzis, R.K., and Pedersen, R. (1998). Centromeric protein B null Mice are viable with no apparent abnormalities. Dev. Biol. *201*, 135-143.

Pidoux, A.L., and Allshire, R.C. (2000). Centromeres: getting a grip of chromosomes. Curr. Opin. Cell Biol. *12*, 308-319.

Pidoux, A.L., and Allshire, R.C. (2004). Kinetochore and heterochromatin domains of the fission yeast centromere. Chrom. Res. *12*, 521-534.

Pidoux, A.L., Choi, E.S., Abbott, J.K.R., Liu, X., Kagansky, A., Castillo, A.G., Hamilton, G.L., Richardson, W., Rappsilber, J., He, X., *et al.* (2009). Fission yeast Scm3: a CENP-A receptor required for integrity of subkinetochore chromatin. Mol. Cell *33*, 299-311.

Politi, V., Perini, G., Trazzi, S., Pliss, A., Raska, I., Earnshaw, W.C., and Valle, G.D. (2002). CENP-C binds the alpha-satellite DNA in vivo at specific centromere domains. J. Cell Sci. *115*, 2317-2327.

Probst, A.V., Dunleavy, E., and Almouzni, G. (2009). Epigenetic inheritance during the cell cycle. Nat. Rev. Mol. Cell Biol. *10*, 192-206.

Santos, F., Peters, A.H., Otte, A.P., Reik, W., and Dean, W. (2005). Dynamic chromatin modifications characterise the first cell cycle in mouse embryos. Dev. Biol. *280*, 225-236.

Sekulic, N., Bassett, E.A., Rogers, D.J., and Black, B.E. (2010). The structure of (CENP-A-H4)2 reveals physical features that mark centromeres. Nature *467*, 347-351.

Shuaib, M., Ouararhni, K., Dimitrov, S., and Hamiche, A. (2010). HJURP binds CENP-A via a highly conserved N-terminal domain and mediates its deposition at centromeres. Proc. Natl. Acad. Sci. *107*, 1349-1354.

Silva, M.C.C., and Jansen, L.E.T. (2009). At the right place at the right time: novel CENP-A binding proteins shed light on centromere assembly. Chromosoma *118*,

567-574.

Smith, K.M., Phatale, P.A., Sullivan, C.M., Pomraning, K.R., and Freitag, M. (2011). Heterochromatin is required for normal distribution of neurospora crassa cenH3. Mol. Cell. Biol. *31*, 2528-2542.

Sullivan, B.A., Blower, M.D., and Karpen, G.H. (2001). Determining centromere identity: cyclical stories and forking paths. Nat. Rev. Genet. *2*, 584-596.

Sullivan, B.A., and Karpen, G.H. (2004). Centromeric chromatin exhibits a histone modification pattern that is distinct from both euchromatin and heterochromatin. Nat. Struct. Mol. Biol. *11*, 1076-1083.

Sullivan, K.F., and Glass, C.A. (1991). CENP-B is a highly conserved mammalian centromere protein with homology to the helix-loop-helix family of proteins. Chromosoma *100*, 360-370.

Sullivan, K.F., Hechenberger, M., and Masri, K. (1994). Human CENP-A contains a histone H3 related histone fold domain that is required for targeting to the centromere. J. Cell Biol. *127*, 581-592.

Verdel, A., Jia, S., Gerber, S., Sugiyama, T., Gygi, S., Grewal, S.I.S., and Moazed, D. (2004). RNAi-mediated targeting of heterochromatin by the RITS complex. Science *303*, 672-676.

Yamagata, K., Yamazaki, T., Miki, H., Ogonuki, N., Inoue, K., Ogura, A., and Baba, T. (2007). Centromeric DNA hypomethylation as an epigenetic signature discriminates between germ and somatic cell lineages. Dev. Biol. *312*, 419-426.

Yamagishi, Y., Sakuno, T., Shimura, M., and Watanabe, Y. (2008). Heterochromatin

links to centromeric protection by recruiting shugoshin. Nature *455*, 251-255.

Yoda, K., Ando, S., Morishita, S., Houmura, K., Hashimoto, K., Takeyasu, K., and Okazaki, T. (2000). Human centromere protein A (CENP-A) can replace histone H3 in nucleosome reconstitution in vitro. Proc. Natl. Acad. Sci. *97*, 7266-7271.

Zhang, K., Mosch, K., Fischle, W., and Grewal, S.I.S. (2008). Roles of the Clr4 methyltransferase complex in nucleation, spreading and maintenance of heterochromatin. Nat. Struct. Mol. Biol. *15*, 381-388.

국문초록 / ABSTACT IN KOREAN

Mis18α는 염색체의 분리를 조절하는 Mis18 복합체중 하나이다. Mis18 복합체는 세포의 분열기 후반부와 이른 G1기 동안에 동원체에 위치하며, 히스톤 단백질 변이체중 하나인 CENP-A의 동원체 이동을, 단백질 상호간의 결합 없이 조정한다고 알려져 있다. 비록 이러한 Mis18α의 라이선싱이나 프라이밍 기능이 세포 분열기에 동원체의 유지에 중요하지만, 그 메커니즘은 대부분 알려지지 않았다. 이에, 본 연구에서는 Mis18α 유전자의 결손 생쥐를 이용하여 개체 발달과정에 있어서 Mis18α의 생리학적 역할을 조사하고, CENP-A 단백질이 동원체로 침착하는 과정을 조절하는 Mis18α의 메커니즘을 확인하였다.

Mis18α 유전자 결손 생쥐는 세포자멸사에 의해 초기 배아 발달과정에서 사멸한다는 사실을 발견하였다. 배아 발달과정중의 3.5일에서 채취한 Mis18α 유전자 결손 배아는 염색체 분리에 심각한 결함을 보이고, 동원체에서 CENP-A가 사라지는 현상을 보인다. 이 배아의 생체 밖 배양실험을 통해, Mis18α 유전자 결손 배아의 경우 내세포집단이 자라지 못하고 세포 사멸에 의해 없어지게 되는 것을 확인하게 되었다. 이러한 배아 발달과정상의 세포자멸사는 Mis18α 유전자 결손에 의해 일어나는, CENP-A 단백질이 동원체에서 사라지는 현상과 염색체의 분리 결함이 누

적되어 발생하게 된다는 사실을 알게 되었다. 이 결과를 뒷받침하기 위해서, Cre 유전자의 주입을 통해서 만든 Mis18α 유전자 결손 섬유아세포(*Mis18α*$^{\Delta/\Delta}$ MEFs)를 이용해 CENP-A 이상과 염색체 분열 결함 현상을 조사하였다. Mis18α 유전자 결손 배아에서와 마찬가지로, *Mis18α*$^{\Delta/\Delta}$ MEFs 세포는 분열기에서의 결함과, CENP-A의 동원체 이동 이상, 그리고 세포자멸사를 보였다. 결과적으로 Mis18α 유전자 결손은 세포분열 상황에서 CENP-A가 동원체에서 사라지게 만들고, 이는 결국 염색체의 분리 결함을 일으키게 된다. 이러한 결함은 초기 배아 발달과정에서 세포자멸사를 가져와 개체의 생성이 불가능하게 된다는 사실을 통해 배아 발달과정에서 Mis18α의 역할을 규명하였다.

CENP-A 와의 결합 없이, CENP-A가 동원체로 이동하는 것을 조절하는 Mis18α의 라이선싱 역할은 동원체의 후성유전학적 조절을 관장함으로써 일어난다는 사실을 확인하였다. 단백질의 라이신기가 메틸화 되거나 아세틸화 되는 히스톤 단백질의 변형은, *Mis18α*$^{\Delta/\Delta}$ MEFs 세포에서 정상보다 줄어들어 있음을 알게 되었다. 또한 동원체에서 발생하게 되는 전사체는 반대로 증가되어 있는 것을 *Mis18α*$^{\Delta/\Delta}$ MEFs 세포에서 발견하였다. 이를 바탕으로, 이러한 히스톤 변형의 감소와 동원체에서 비롯된 전사체의 증가를 조절하는 효소들 중에서 Mis18α와 결합할 수 있는 단백질을 찾아본 결과, DNA 메틸화 효소인 DNMT3A/3B가 Mis18α의 LRR 부위에

결합한다는 사실을 확인하게 되었다. 이러한 상호간의 결합을 통해 Mis18α 결손 MEFs 세포에서는 동원체에 위치하는 DNMT3A/3B 가 줄어들어 있는 것을 알게 되었고, 이 현상은 정상 Mis18α 단백질의 주입으로 복원이 되지만 DNMT3A/3B 와 결합하지 못하는 변이 Mis18α 단백질로는 복원되지 않는다는 사실도 확인하였다. 결국, Mis18α와 DNMT3A/3B 단백질은 상호간의 동원체 이동을 강화하는 역할을 작용을 한다는 사실 또한 확인하게 되었다. 다음으로 DNA 메틸화 효소의 변화가 가져오는 차이를 확인하기 위해 bisulfite를 이용한 염기서열 분석법을 수행하였다. 이를 통해, Mis18α 유전자 결손이 DNMT3A/3B 단백질의 동원체 이동을 줄여서 동원체 DNA의 메틸화를 정상보다 낮추게 된다는 사실을 밝혔다. 그러므로 Mis18α의 라이선싱 기능은 DNMT3A/3B 와의 결합으로부터 형성되고, 동원체 DNA의 메틸화를 유지하는 역할을 수행해 CENP-A의 동원체 이동을 유지하게 된다.

결론적으로, 세포 분열시에 CENP-A의 동원체로의 이동과 유지는, Mis18α/DNMT3A/3B에 의한 동원체 DNA 부분의 후성유전학적 메틸화 조절을 통해서 이루어지게 된다는 사실을 본 연구를 통해 규명하였다. 또한, CENP-A 이동을 관장하는 Mis18α의 이러한 후성유전학적 조절은 결국 Mis18α의 라이선싱 기능이 동원체라는 구조를 특정하고 유지하게 한다는 사실을 실험적으로 확인하였다.

주요어

Mis18α/ DNMT3A/ DNMT3B/ CENP-A/ 동원체/ 세포 분열기/ 염색체 분리/ 히스톤 변형/ DNA 메틸화/ 후성유전학적 조절